

Oligocene and Lower Miocene Siliceous Microfossil Biostratigraphy of Cape Roberts Project Core CRP-2/2A, Victoria Land Basin, Antarctica

R.P. SCHERER^{1*}, S.M. BOHATY² & D.M. HARWOOD³

¹Department of Geology and Environmental Geosciences, Northern Illinois University, DeKalb, IL 60115 - USA

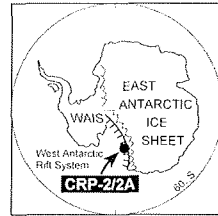
²Department of Earth Sciences, University of California, Santa Cruz, CA 95064 USA

³Department of Geosciences, University of Nebraska-Lincoln, Lincoln, NE 68588-0340 - USA

*Corresponding author (reed@geol.niu.edu)

Received 6 October 1999; accepted in revised form 10 July 2000

Abstract - Marine diatoms are the primary biostratigraphical and palaeoenvironmental tool for interpreting the upper Palaeogene and lower Neogene strata recovered during the second drilling season of the Cape Roberts Project at site CRP-2 in the western Ross Sea, Antarctica. Silicoflagellates, ebridians, and a chrysophyte cyst provide supporting biostratigraphical information. More than 100 dominantly planktic diatom taxa are recognised. Of these, more than 30 are treated informally, pending SEM examination and formal description. Many other taxa are noted only to generic level. Lower Oligocene (*c.* 31 Ma) through lower Miocene (*c.* 18.5 Ma) diatoms occur from 28 mbsf down to 565 mbsf. Below this level, to the bottom of the hole at 624.15 mbsf, diatom assemblages are poorly-preserved and many samples are barren. A biostratigraphic zonal framework, consisting of ten diatom zones, is proposed for the Antarctic continental shelf. Ages inferred from the diatom biostratigraphy correspond well with geochronological data from argon dating of volcanic materials and strontium dating of calcareous macrofossils, as well as nannofossil biochronological datums. The biochronostratigraphical record from CRP-2/2A provides an important record of diatom events and mid-Cenozoic environmental changes in the Antarctic neritic zone.



INTRODUCTION

Diatom biostratigraphy on the Antarctic continental shelf has developed progressively over the past 25 years since the initial recovery of lower Miocene to Pleistocene diatom-bearing sections during DSDP Leg 28 (McCollum, 1975). Although a Southern Ocean biochronological framework advanced rapidly as a result of ODP legs 113, 114, 119, and 120, diatom assemblages on the continental shelf are sufficiently different from Southern Ocean floras to require a separate zonal scheme. The limited number of stratigraphic sections on the Antarctic shelf has prevented biochronology in this region from progressing at the same pace as the Southern Ocean. Moreover, stratigraphic complexities associated with fossil reworking, the presence of numerous hiatuses, sections with a high component of clastic sediment, and extremely variable sediment accumulation rates, all influenced to some degree by glacial processes, make the construction of a biochronological framework difficult. The process of documenting the fossil occurrences, describing new taxa, and calibrating biostratigraphic events to a global time scale is underway. The CRP drillcores, especially the CRP-2/2A drillcore, provide materials needed to advance siliceous microfossil biochronology. The zonation proposed here will be tested, refined and applied with the recovery of future stratigraphic sections.

The Cape Roberts Project (CRP) is an international drilling effort with the goals of recovering a tectonic and paleoenvironmental history of the Victoria Land Basin, Western Ross Sea, Antarctica. A thick sequence (624.15 m)

of glacial, glacial-marine, and hemipelagic sediment was recovered in the CRP-2/2A drillcore during the second drilling season of the Cape Roberts Project. This stratigraphic section includes *c.* 26 m of Pliocene and Quaternary strata, *c.* 150 m of lower Miocene strata, *c.* 120 m of upper Oligocene strata, and *c.* 320 m of lower Oligocene strata (Wilson et al., this volume). The occurrence and biostratigraphical utility of siliceous microfossils (diatoms, silicoflagellates, ebridians, chrysophycean cysts) in the Miocene and Oligocene section of the CRP-2/2A drillcore is the focus of the present report. It represents an update of initial results reported during the drilling season (CRP Science Team, 1999). A report on the siliceous microfossil assemblages in Pliocene/Pleistocene section of CRP-2/2A was presented in the Initial Reports volume (CRP Science Team, 1999); diatom assemblages present in this interval are not treated here.

Siliceous microfossils occur in variable abundance through the stratigraphic section in the CRP-2/2A drillcore (Fig. 1). Diatoms are most abundant in fine-grained lithologies, except in intervals that have undergone significant diagenesis. Some relatively coarse, sandy intervals, however, also contain abundant diatoms (*e.g.* *c.* 135 mbsf). Radiolarians, including fragments, are nearly absent from the recovered sequence. More than 100 diatom species and species groups, plus 9 silicoflagellates, 4 ebridians, 3 endoskeletal dinoflagellates, and one biostratigraphically-useful chrysophyte cyst are recognised in Oligocene and lower Miocene samples from CRP-2/2A.

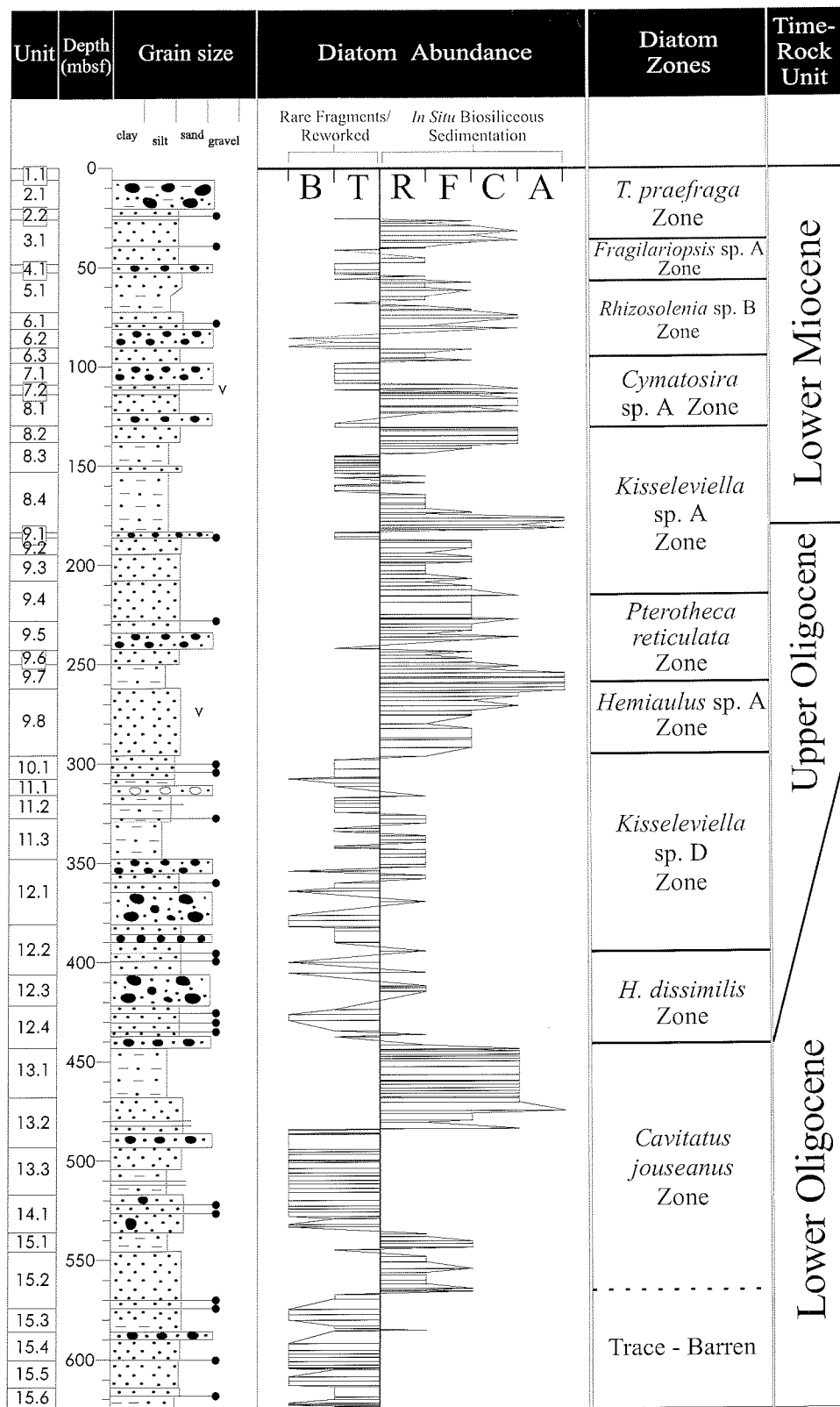


Fig. 1 - Diatom abundance and proposed zonation for lower Oligocene-lower Miocene sediments of CRP-2/2A, plotted against the lithological summary log. Abundance categories (B = barren; T = trace; R = rare; F = frequent; C = common; A = abundant) are based on analysis of strewn slides of unsieved material.

METHODS

CRP-2/2A samples were prepared for siliceous microfossils as strewn-slides of raw sediment, following standard procedures. As necessary, selected samples were

reacted in H_2O_2 and/or HCl to remove organic material and carbonate cements, respectively. Additional samples were further prepared by separating the >10mm fraction using nylon screens. Several samples were sieved with 20 μ m and 25 μ m stainless steel mesh sieves. Diatoms

from 15 samples were concentrated through heavy-liquid density separation techniques, using a 2.2 specific gravity sodium polytungstate solution. Concentration by sieving was particularly helpful to recover whole specimens of marker taxa in intervals characterised by a high degree of diatom fragmentation (see Harwood et al., 1989a).

Stratigraphical occurrence and abundance data are based on detailed analysis of more than 50 diatom-bearing samples, plus examination of more than 250 additional samples (Tab. 1). Diatom assemblages identified in LM examination of 39 samples are presented in table 2. These samples are considered to be a representative sub-set of all diatom-rich samples examined. Samples with very low diatom abundance are not presented, nor are all closely-spaced samples examined from diatom-rich intervals. Text and figures may present data from samples not included in table 2. For example, the first (lowest) occurrence (FO) and last (highest) occurrence (LO) of *Lisitzinia ornata* are listed in the text, table 3, and figure 3, as 266.38 and 259.21, respectively, although neither of these samples is listed in table 2. Table 2 lists samples 264.38 and 260.02, which are representative of the interval containing *Lisitzinia ornata*.

Diatom Abundance per Sample

Relative diatom abundance, represented graphically on figure 1 and in table 1, was determined from strewn slides of unsieved material. Total abundance of diatoms was determined following the criteria outlined below. These estimates were made by performing several traverses across a 20x40 mm cover slip at 750x magnification and include an interpretation that attempts to distinguish reworked assemblages from *in situ* biosiliceous sedimentation. Sample assigned "rare" to "abundant" estimates contain complete, well-preserved valves. Due to high degree of fragmentation in many samples, the amount of fine-grained biosiliceous material was also considered in these overall abundance estimates.

B = Barren: no diatom valves or fragments present.

T = Trace/ Reworked: rare fragments present.

R = Rare: 1 complete valve in 5-30 fields of view.

F = Frequent: 1 complete valve in 1-5 fields of view.

C = Common: 2-5 complete valves per field of view (or "frequent" occurrence with a significant component of the silt and clay-sized fraction composed of biosiliceous material).

A = Abundant: >5 complete valves per field of view (or "common" occurrence with most of the silt and clay-sized fraction composed of biosiliceous material).

Relative Abundance of Individual Taxa

Abundance of individual taxa (Tab. 2) was estimated at 750x magnification from several preparations (raw sample strewn, smear slide, sieved, etc.). These assignments were made as follows:

r = reworked or redeposited.

fr = Rare fragment(s) of taxon noted.

X = Present: complete specimens rare (<1 per traverse).

R = Rare: 1 specimen in 5-30 fields of view.

F = Frequent: 1 specimen in 1-5 fields of view.

C = Common: 1 specimen in every field of view.

A = Abundant: ≥2 specimens per field of view.

Age assignments and diatom taxonomy are based on a large body of literature from the Southern Ocean, the Antarctic continental shelf, and other areas. Key Southern Ocean biostratigraphical datums are reviewed, and ages are recalibrated to the Berggren et al. (1995) time scale. The main sources of diatom biostratigraphical information for CRP-2/2A are the reports from Southern Ocean drilling, notably Hajós (1976), Schrader (1976), Gombos (1977), Gombos & Ciesielski (1983), Baldauf & Barron (1991), Harwood & Maruyama (1992), and the compilation of Ramsay & Baldauf (1999). Useful diatom reports from Antarctic continental shelf drilling and piston coring include McCollum (1975), Harwood (1986), Harwood (1989), Harwood et al. (1989a), Harwood et al. (1998), Barron & Mahood (1993), Mahood et al. (1993), and Harwood & Bohaty (2000). Several reports from stratigraphical sections outside of the Antarctic region also contributed useful information (Akiba et al., 1993; Gladenkov & Barron, 1995; Scherer & Koç, 1996; Schrader & Fenner, 1976; and Yanagisawa & Akiba, 1998). Due to space limitations, only short-form synonomies are presented in the taxonomic section, with concentration on biostratigraphically-significant taxa. Occurrence data for several groups of long-ranging taxa, and those with uncertain taxonomic divisions are combined in table 2 at the genus level (e.g. *Stephanopyxis* spp. and *Coscinodiscus* spp.). Many benthic taxa are similarly reported only to the genus level (e.g. *Cocconeis* spp., *Diploneis* spp., *Grammatophora* spp., *Hyalodiscus* spp., *Odontella* spp. and *Rhabdonema* spp.).

CRP-2/2A siliceous microfossil data (Fig. 2, Tab. 2) include many informal taxonomic designations. These designations are internal to this report on CRP-2/2A unless specific reference is made to published works (e.g., *Hemiaulus* sp. A of Harwood, 1986). Important undescribed taxa referred to in the text are illustrated, discussed and informally described. Formal proposal and description of these taxa will follow in subsequent papers.

DEVELOPMENT OF AN ANTARCTIC CONTINENTAL SHELF DIATOM ZONATION

Sediments recovered from CRP-2/2A allow further development of the diatom biostratigraphical zonation for the Antarctic continental shelf, and represent a significant advancement, building upon initial efforts in this region (Harwood, 1986; 1989). The nearly 600 m of lower Miocene and Oligocene sediment recovered include significant diatom floral overturn, allowing subdivision into 10 diatom biozones (Fig. 2, Tab. 2, 3). Two of the zonal boundaries are tied to, or are correlated with, the magnetostratigraphically-calibrated Southern Ocean diatom biozonation.

At least three major unconformities and numerous minor unconformities are present through the sequence (Wilson et al., this volume). Approximately 6 million years of the ~13 m.y. interval represented in CRP-2/2A is

Tab. 1 - CRP-2/2A relative diatom abundance data.¹

CRP-2			182.17	182.17	C	405.58	405.59	B
25.25	25.26	T	183.58	183.59	T	412.27	412.29	R
26.48	26.49	F	185.76	185.77	T	413.05	413.06	R
26.78	26.79	R	186.70	186.71	T	414.79	414.80	R
27.70	27.71	R	187.67	187.68	F	424.10	424.11	T
28.90	28.92	R-F	188.57	188.58	F	426.49	426.50	B
29.06	29.08	R	191.36	191.37	F	429.38	429.39	B
31.71	31.72	F-C	193.99	194.00	R	434.66	434.67	T
33.84	33.85	F	195.70	195.71	F	436.72	436.73	R
36.24	36.25	C	197.12	197.13	F	437.68	437.69	T
36.40	36.41	F	198.52	198.53	F	441.85	441.86	R-F
37.44	37.45	F	199.08	199.09	R	443.89	443.90	C
39.82	39.83	R	200.16	200.17	R	444.25	444.26	F
40.24	40.25	R	202.85	202.86	R	446.96	446.99	C
41.19	41.20	T	204.58	204.59	R	446.55	446.56	C
45.12	45.13	R	206.81	206.82	F	447.68	447.69	C
47.41	47.51	R	208.76	208.77	R	448.73	448.74	C
47.82	47.83	T	210.58	210.59	F	450.06	450.07	C
50.82	50.83	T	212.61	212.62	F	453.19	452.20	C
52.47	52.48	T	215.33	215.34	C	456.83	456.84	C
54.36	54.37	R	215.72	215.73	F	459.70	459.71	C
56.10	56.11	R	218.80	218.81	F	459.90	459.91	C
57.32	57.42	F	224.84	224.84	F	460.13	460.14	C
CRP-2A			226.61	226.61	F	461.65	461.66	C
53.19	53.20	T	226.94	226.95	F	463.53	463.54	C
55.81	55.82	T	227.27	227.29	C	464.98	465.00	C
58.15	58.16	R	229.70	229.71	F	466.27	466.28	C
59.96	59.97	R	231.49	231.50	F	467.85	467.86	C
61.50	61.51	F	233.00	233.01	F	468.52	468.53	C
64.60	64.61	R	234.70	234.71	R	470.79	470.80	C
66.24	66.25	R	236.25	236.26	C	474.90	474.91	A
67.84	67.85	T	237.87	237.88	F	476.30	476.31	F
69.47	69.48	R	241.89	241.90	T	479.71	479.72	F
71.13	71.14	F	243.63	243.64	F	480.82	480.83	R
71.70	71.71	F	245.54	245.55	R	483.92	483.93	C
73.94	73.95	C	247.08	247.09	F	484.55	484.56	B
75.52	75.56	C	249.07	249.08	F	486.28	486.30	B
79.48	79.49	R	250.93	250.94	C	486.76	486.77	B
80.65	80.68	C	252.46	252.47	F	494.38	494.39	B
80.79	80.80	F	254.43	254.44	A	495.62	495.63	B
85.57	85.58	B	256.40	256.43	A	496.90	496.91	B
87.58	87.59	T	256.91	256.92	A	499.65	499.66	B
89.72	89.73	B	259.20	259.21	A	500.26	500.27	B
90.77	90.78	T	260.02	260.04	A	501.05	501.06	B
91.19	91.20	F	261.60	261.61	A	503.90	503.91	B
93.04	93.05	R	263.20	263.21	A	506.22	506.23	B
95.61	95.62	R	264.38	264.39	C	507.86	507.88	B
96.70	96.85	F	266.38	266.39	C	510.13	510.14	B
96.84	96.85	R	268.31	268.32	F	511.75	511.76	B
98.30	98.31	T	271.02	271.04	C	514.04	514.05	B
101.17	101.18	T	273.50	273.51	F	516.08	516.09	B
103.28	103.29	T	275.48	275.49	F	520.12	520.13	B
106.77	106.78	T	275.90	275.91	F	523.04	523.05	B
108.18	108.19	T	280.12	280.13	R	524.39	524.41	B
109.12	109.13	F	282.42	282.43	F	526.01	526.02	B
111.05	111.06	C	287.07	287.08	F	528.22	528.23	B
111.53	111.54	T	288.00	288.01	F	529.33	529.34	T
112.90	112.91	F	292.08	292.09	F	532.34	532.35	B
113.51	113.52	C	296.39	296.40	R	533.43	533.44	B
114.43	114.44	F	298.07	298.08	T	537.25	537.26	R
116.15	116.16	C	302.65	302.66	T	538.46	538.47	R
119.65	119.66	C	306.95	306.96	T	540.73	540.74	F
120.33	120.34	F	307.70	307.71	B	542.04	542.05	F
122.56	122.57	C	309.88	309.89	T	543.81	543.83	F
123.32	123.33	R	311.56	311.57	T	545.18	545.19	T
128.52	128.53	T	316.48	316.50	R	548.57	548.58	R
130.32	130.33	T	317.27	317.28	T	551.29	551.30	R
130.90	130.93	C	318.85	318.86	T	554.70	554.71	F
131.67	131.68	C	320.05	320.06	T	556.60	556.61	R
132.34	132.35	C	322.00	322.01	T	557.85	557.86	R
134.74	134.75	C	324.54	324.55	T	560.33	560.34	R
135.09	135.10	C	326.07	326.08	R	562.31	562.32	R
137.46	137.47	C	328.08	328.09	R	564.63	564.66	F
138.83	138.84	C	330.08	330.09	R	565.50	565.51	R
139.90	139.91	F	332.76	332.77	T	565.98	565.99	F
141.26	141.27	F	334.14	334.15	T	567.50	567.51	T
143.69	143.70	R	336.51	336.52	R	570.02	570.03	T
145.14	145.15	T	338.45	338.46	R	575.15	575.16	B
145.58	145.59	T	339.80	339.82	R	577.67	577.68	B
147.07	147.08	T	341.72	341.73	T	580.53	580.54	B
148.19	148.20	T	342.46	342.47	T	583.51	583.52	T
148.72	148.73	T	343.26	343.27	R	584.54	584.57	T
149.65	149.66	T	345.58	345.59	R	585.58	585.59	R
150.70	150.71	T	347.31	347.32	R	585.84	585.85	T
152.40	152.41	T	350.89	350.90	R	592.23	592.24	B
153.70	153.71	T	352.15	352.16	R	595.72	595.73	B
155.20	155.21	R	354.23	354.24	B	597.44	597.45	B
156.07	156.08	T	356.44	356.45	T-R	599.25	599.26	B
158.50	158.51	R	358.22	358.24	T-R	601.35	601.36	B
159.81	159.82	T	360.27	360.28	T	603.14	603.15	B
160.29	160.30	T	362.91	362.92	T	604.40	604.42	B
162.42	162.43	T	364.27	364.28	B	604.92	604.93	B
164.50	164.51	R	369.73	369.74	R	605.66	605.67	T
166.34	166.35	R	376.54	376.55	B	609.07	609.08	B
168.79	168.80	R	379.03	379.04	B	611.10	611.11	B
169.58	169.59	R	382.02	382.03	B	613.35	613.36	B
171.49	171.50	R	382.81	382.82	T	614.03	614.04	T
173.46	173.47	F	384.28	384.29	T	619.19	619.20	T
174.38	174.39	R	390.01	390.02	T	620.50	620.51	T
176.29	176.30	A	390.19	390.21	T	622.31	622.32	B
177.89	177.90	A	394.48	394.49	R	623.03	623.04	B
179.93	179.94	C	400.22	400.23	B	623.76	623.79	T
181.32	181.33	A	405.37	405.38	R-F	624.03	624.04	T

¹All depths are in metres below sea floor (mbsf). Samples 25.25 through 57.32 mbsf, above the solid line, are from Hole CRP-2. Samples from 53.19 through 624.03 mbsf, below the solid line, are from Hole CRP-2A. The two numbers represent top and bottom depth of each sample (mbsf). The letter code indicates total diatom abundance, as defined in the text: B = barren, T = trace, R = rare, F = frequent, C = common, and A = abundant.

Tab. 2 - Occurrence data for diatoms, silicoflagellates, ebridians and stratigraphically important chrysophyte cysts in CRP-2/2A. Data for rare taxa not reported here is included in the section on systematic palaeontology.

Taxon	Sample Depth (mbst)	Diatoms	Ecdology	Total Abundance	Diatom Preservation
	28.90-92	R-F	P		
	31.71-72	F-C	M	P	
	35.24-25	C	M-A	P	
	47.41-51	R	P	X	
	57.32-42	F	M	P	
	61.50-51	F	P-M	P-B	
	71.13-14	F	M	P	
	75.52-56	C	M	P	
	80.65-68	C	G	P-B	
	96.70-85	F	P	P-B	
	111.05-106	C	G	P	
	122.56-57	C	G	P	
	130.90-93	C	M	P	
	158.80-51	R	P	P	
	177.89-90	A	M	P	
	181.32-33	A	M	P	
	195.70-71	F	M	P-B	
	215.72-73	F	M	P-B	
	236.25-26	C	M	P-B	
	260.02-04	A	M-G	P	
	264.38-39	C	M	P	
	271.02-04	C	G	P	
	292.08-09	F	M	-	
	296.39-41	R	P	P	
	316.48-50	R	P	-	
	326.07-49	R	P	-	
	330.08-10	R	P	-	
	339.80-82	R	P	-	
	345.58-60	R	P	-	
	350.89-90	R	P	-	
	356.44-45	R-R	P	-	
	369.73-75	R	P	-	
	380.19-21	T	P	-	
	394.48-50	R	P	-	
	405.53-59	R-F	P	-	
	412.27-29	R	P	-	
	413.05-414.30	R	P	-	
	436.72-437.37	R	P	-	
	441.85-87	R-F	P	-	
	443.89-90	C	M	P	
	444.95-99	C	M	P	
	464.98-00	C	G	P	
	483.92-93	C	M	P	
	543.81-83	F	M	P	
	564.93-96	F	P	P	
	584.54-57	T	P	-	
	623.76-79	T	P	-	

Tab. 2 - Continued.

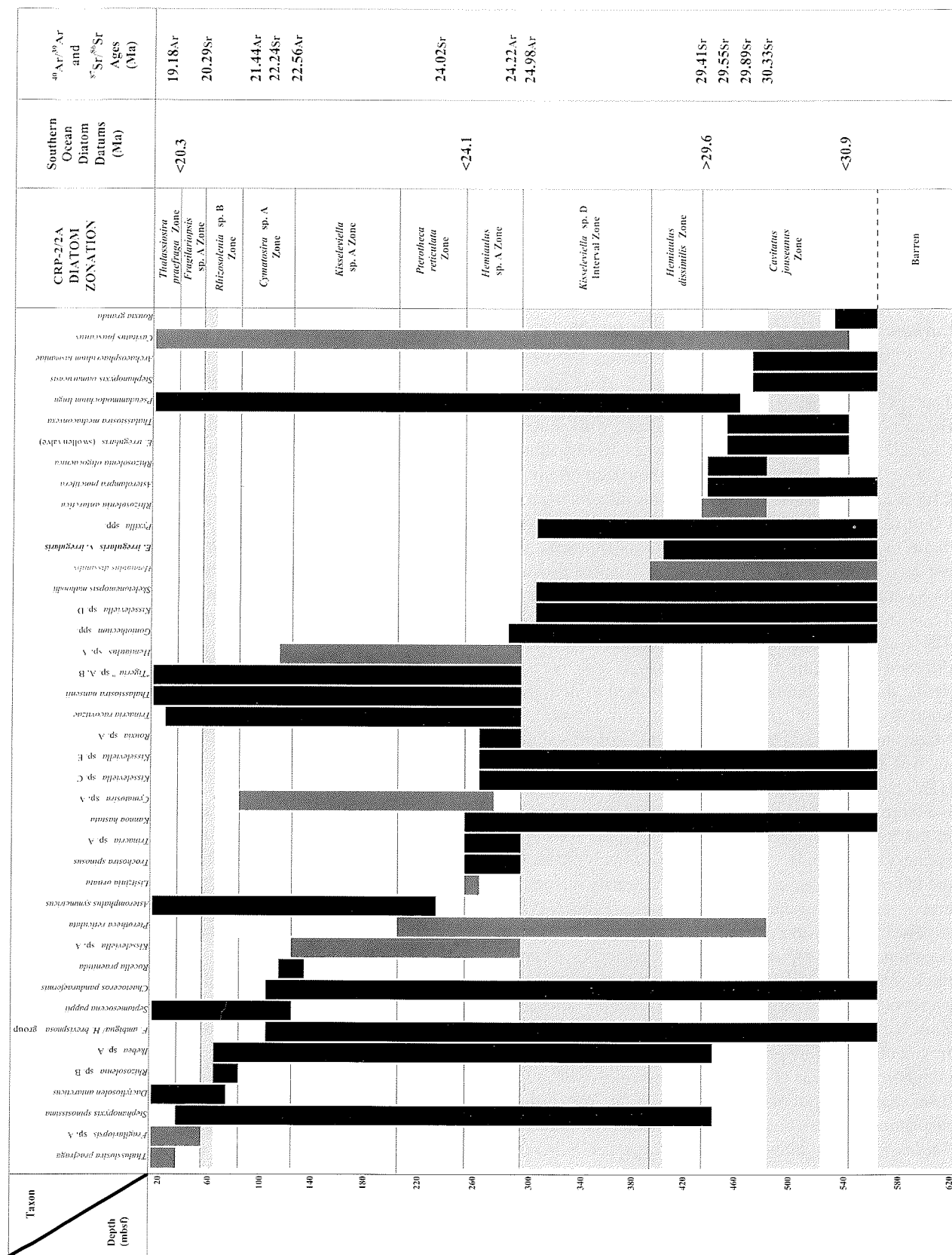


Fig. 2. Stratigraphical ranges of key diatoms and diatom species groups, ebridians, silicoflagellates and chrysophyte cysts in CRP-2/A, scaled according to approximate depth. The chart is a graphical representation of selected taxa from total taxonomic census data (Tab. 2), illustrating the first and/or last consistent occurrences of these taxa within CRP-2/A. These ranges are the foundation for a zonal scheme, presented to the right. Shaded areas reflect poor biosiliceous preservation. Deep-sea biostratigraphical ties and chronostratigraphical determinations based on Sr/Sr and Ar/Ar dates (Lavelle, this volume; McIintosh, this volume) are presented on the far right.

missing in these hiatuses. Consequently, it is not known how much biostratigraphical information is missing, as numerous diatom ranges truncate at these boundaries. Future Antarctic continental shelf drilling will reveal the details of these lower Oligocene to lower Miocene biostratigraphical events that are not represented in the CRP-2/2A core. The proposed continental shelf diatom zones presented in table 3 and discussed below in the context of the CRP-2/2A drillcore.

CRP-2/2A WORKING DIATOM ZONATION

Cavitatus jouseanus Concurrent Range Zone, lower Oligocene (this report)

Top: LO of *Rhizosolenia antarctica*, 441.85 mbsf.
Bottom: FO of *Cavitatus jouseanus*, below the base of CRP-2/2A and down to 48.44 mbsf in the CRP-3 drillhole.

The *Cavitatus jouseanus* concurrent Zone in CRP-2/2A is defined as the stratigraphic interval from the FO of *Cavitatus jouseanus* up to the LO of *Rhizosolenia antarctica*. The basal range of *Cavitatus jouseanus* was not recovered in CRP-2/2A, but it was noted down to 44.83 mbsf in the CRP-3 drillcore (Cape Roberts Science Team, 2000.), below the interval recovered by CRP-2/2A. The *Cavitatus jouseanus* Zone proposed here uses a different datum (the LO of *Rhizosolenia antarctica*) to define the upper boundary, than that used to define the Southern Ocean *C. jouseanus* Zone of Harwood & Maruyama (1992). The FO of *Rocella vigilans* var. A is applied as the upper boundary of the *C. jouseanus* Zone (Harwood & Maruyama, 1992). *Rhizosolenia antarctica* is a large, heavily silicified diatom, previously employed in the Southern Ocean as a biostratigraphic marker by Fenner (1984, 1985). The base of this zone is not strong; the FO of *C. jouseanus* is difficult to identify due to rare and sporadic occurrence in its lower range (Fenner, 1984).

The *C. jouseanus* Zone includes two intervals of diatom occurrence at the top and base of this zone (Fig. 1) and a thick interval (533.44 to 486.28 mbsf) of poor diatom preservation. Assemblages in the *Cavitatus jouseanus* Zone of CRP-2/2A are characterised by rare, often fragmented specimens of *C. jouseanus* and relatively common specimens of *Skeletonemopsis mahoodii*. Other taxa characteristic of this zone include *Rhizosolenia antarctica*, *Kannoahastata*, *Goniothecium odontella*, rare *Thalassiosira mediaconvexa* (late form, see Scherer & Koç, 1996), and rare *Rhizosolenia oligocaenica*. Rare examples of very small specimens of *Distephanosira architecturalis*, which are known from sediments of early Oligocene age (Scherer & Koç, 1996), are also noted. Additionally, rare occurrences of *Kisseleviella* sp. G, a form recorded in CIROS-1 as *K. carina* (Harwood, 1989, pl. 4, fig. 37), are also noted in this zone. Many of the rare occurrences of upper Eocene – lower Oligocene diatoms may be reworked; palynomorphs suggest a significant amount of reworking in this interval (Askin et al., this volume; Hannah et al., this volume). Several taxa truncate near the top of this zone, including *Asterolamprapunctifera*, *Rhizosolenia oligocaenica*, and *Thalassiosira*

mediaconvexa. These truncations may represent a preservational bias, due to poor preservation and low abundance in the overlying interval.

The lowermost interval of moderately preserved diatoms in CRP-2/2A occurs from 564.66 to 543.83 mbsf in the *Cavittatus jouseanus* Zone. These assemblages are characterised by *Skeletonemopsis mahoodii*, *Stephanopyxis omaruensis*, rare *Rouxia granda*, and the chrysophyte-cyst *Archaeosphaeridium tasmaniae*. Below this interval, the lowermost 50 m of CRP-2/2A (624.03 - 565.50 mbsf) contains only rare, recrystallised diatoms.

Hemiaulus dissimilis Partial Range Zone, lower Oligocene (this report).

Top: LO of *Hemiaulus dissimilis*, 394.48 mbsf.
Bottom: LO of *Rhizosolenia antarctica*, 441.85 mbsf.

The *Hemiaulus dissimilis* Zone is defined as the stratigraphic interval from the LO of *Rhizosolenia antarctica* up to the LO of *Hemiaulus dissimilis*. Diatoms within this zone are poor to moderately preserved, and occur in low abundance (Fig. 1). The lower part of the zone includes the LO of *Eurossia irregularis v. irregularis*, which occurs as fragments up to 412.27 mbsf. Rare specimens of *H. dissimilis* are noted further up the section (e.g. 316.46 mbsf). These occurrences are interpreted to represent reworked specimens.

Kisseleviella sp. D Interval Zone, upper Oligocene (this report)

Top: FO of *Hemiaulus* sp. A of Harwood (1986), 296.41 mbsf.
Bottom: LO of *Hemiaulus dissimilis*, 394.48 mbsf.

The *Kisseleviella* sp. D Zone is defined as the stratigraphical interval from the LO of *Hemiaulus dissimilis* up to the FO of *Hemiaulus* sp. A. In CRP-2/2A, this zone is represented by poor preservation and low abundance, including intervals that are barren of siliceous microfossils (Fig. 1). The nominative taxon of this zone, *Kisseleviella* sp. D, is present, but rare, throughout the zone.

Hemiaulus sp. A Concurrent Range Zone, upper Oligocene (this report)

Top: LO of *Lisitzinia ornata*, 259.21 mbsf.
Bottom: FO of *Hemiaulus* sp. A of Harwood (1986), 296.41 mbsf.

The *Hemiaulus* sp. A Concurrent Range Zone is defined as the stratigraphical interval from the FO of *Hemiaulus* sp. A up to the LO of *Lisitzinia ornata*. In CRP-2/2A, the lower boundary of this zone at 296.41 is truncated by an interval of poor preservation. The FOs of several taxa are coincident with this change in preservation, including *Trinacria* sp. A, *Kisseleviella* sp. A, *Thalassiosira nansenii*, and "Tigeria" spp. Other distinctive taxa within this zone include *Cymatosira* sp. A, *Trochosira spinosus*, *Kisseleviella* sp. B, and rare *Rouxia* sp. A. From c. 265 to 255 mbsf, a strong pulse of biosiliceous sedimentation is noted in the upper part of this zone, which extends into the overlying *Pterotheca reticulata* Zone (Fig. 1). *Lisitzinia*

Tab. 3 - Definition of boundaries for CRP2/2A diatom zonation and characteristic taxa of each zone.

Zone	Boundaries	CRP-2/2A Depth (mbsf)	Characteristic Taxa
<i>Thalassiosira praefraga</i> Range Zone	Top. LO <i>Thalassiosira praefraga</i> Base. FO <i>Thalassiosira praefraga</i> *	Unconformity at c. 28 mbsf 36.25	<i>Dactyliosolen antarcticus</i> <i>Fragilariopsis</i> sp. A <i>Thalassiosira nansenii</i> <i>Thalassiosira praefraga</i> <i>Dactyliosolen antarcticus</i> <i>Fragilariopsis</i> sp. A
<i>Fragilariopsis</i> sp. A Partial Range Zone	Top. FO <i>Thalassiosira praefraga</i> * Base. FO <i>Fragilariopsis</i> sp. A	36.25 57.42	
<i>Rhizosolenia</i> sp. B Interval Zone	Top. FO <i>Fragilariopsis</i> sp. A Base. LO <i>Cymatosira</i> sp. A	57.42 96.70	<i>Ikebea</i> sp. A <i>Rhizosolenia</i> sp. B <i>Septamocena pappii</i> <i>Thalassiosira nansenii</i>
<i>Cymatosira</i> sp. A Partial Range Zone	Top: LO <i>Cymatosira</i> sp. A Base: LO <i>Kisseleviella</i> sp. A	96.70 130.90	<i>Cymatosira</i> sp. A <i>Ikebea</i> sp. A <i>Pseudotriceratium radiosoreticulatum</i>
<i>Kisseleviella</i> sp. A Partial Range Zone	Top. LO <i>Kisseleviella</i> sp. A Base. LO <i>Pterotheca reticulata</i>	130.90 215.72	<i>Cymatosira</i> sp. A <i>Hemiaulus</i> sp. A <i>Kisseleviella</i> sp. A <i>Pterotheca reticulata</i>
<i>Pterotheca reticulata</i> Partial Range Zone	Top. LO <i>Pterotheca reticulata</i> Base. LO <i>Lisitzinia ornata</i> *	215.72 259.21	<i>Asteromphalus symmetricus</i> <i>Cymatosira</i> sp. A <i>Kisseleviella</i> sp. A
<i>Hemiaulus</i> sp. A Concurrent Range Zone	Top. LO <i>Lisitzinia ornata</i> * Base. FO <i>Hemiaulus</i> sp. A	259.21 296.38	<i>Cymatosira</i> sp. A <i>Hemiaulus</i> sp. A <i>Kanno</i> <i>hastata</i> <i>Kisseleviella</i> sp. A <i>Kisseleviella</i> sp. B <i>Rouxia</i> sp. A <i>Pterotheca reticulata</i> <i>Trinacria</i> sp. A <i>Trochosira spinosus</i>
<i>Kisseleviella</i> sp. D Interval Zone	Top. FO <i>Hemiaulus</i> sp. A Base. LO <i>Hemiaulus dissimilis</i>	296.38 394.48	<i>Kisseleviella</i> sp. D <i>Trochosira spinosus</i>
<i>Hemiaulus dissimilis</i> Partial Range Zone	Top. LO <i>Hemiaulus dissimilis</i> Base. LO <i>Rhizosolenia antarctica</i>	394.48 441.85	<i>E. irregularis</i> v. <i>irregularis</i> <i>Hemiaulus dissimilis</i> <i>Kanno</i> <i>hastata</i> <i>Kisseleviella</i> sp. C <i>Kisseleviella</i> sp. D <i>Pyxilla reticulata</i>
<i>Cavittatus jouseanus</i> Concurrent Range Zone	Top. LO <i>Rhizosolenia antarctica</i> Base. FO <i>Cavittatus jouseanus</i> *	441.85 Below CRP-2/2A	<i>Archaeosphaeridium tasmaniae</i> <i>Asterolampra punctifera</i> <i>E. irregularis</i> v. <i>irregularis</i> <i>E. irregularis</i> v. <i>irregularis</i> (elevated valve) <i>Goniothecium odontella</i> <i>Hemiaulus dissimilis</i> <i>Hemiaulus</i> sp. C <i>Kanno</i> <i>hastata</i> <i>Kisseleviella</i> sp. C <i>Kisseleviella</i> sp. D <i>Pseudotriceratium radiosoreticulatum</i> <i>Pyxilla reticulata</i> <i>Rhizosolenia oligocaenica</i> <i>Rhizosolenia antarctica</i> <i>Rouxia granda</i> <i>Skeletonenopsis mahoodii</i>

* Represents a zonal boundary datum tied to the Southern Ocean chronostratigraphy

ornata occurs in this interval of high diatom abundance, although it is rare in this diverse and well-preserved diatom-bearing interval.

Pterotheca reticulata Partial Range Zone, upper Oligocene (this report)

Top: LO of *Pterotheca reticulata*, 215.74 mbsf.
Bottom: LO of *Lisitzinia ornata*, 259.21 mbsf.

The *Pterotheca reticulata* Partial Range Zone is defined as the stratigraphical interval from the LO of *Lisitzinia ornata* up to the LO of *Pterotheca reticulata*. Diatoms are abundant and well-preserved in the lowermost part of this zone. Characteristic taxa of this zone include *Cymatosira* sp. A, *Hemiaulus* sp. A, *Kisseleviella* sp. A, *Cavittatus jouseanus*, *Thalassiosira nansenii*, "Tigeria" spp., several species of *Trinacria*, and *Pterotheca reticulata*. Diatom abundance and diversity is generally lower in the upper

part of the *P. reticulata* Zone, from 259.21 to the top of the zone at 215.74 mbsf.

Kisseleviella sp. A Partial Range Zone, lower Miocene/upper Oligocene (this report)

Top: LO of *Kisseleviella* sp. A, 130.90 mbsf.

Bottom: LO of *Pterotheca reticulata*, 215.72 mbsf.

The *Kisseleviella* sp. A Partial Range Zone is defined as the stratigraphical interval from the LO of *Pterotheca reticulata* up to the LO of *Kisseleviella* sp. A. In CRP-2/2A, this zone is characterised by generally high, but variable diatom abundance (Fig. 1). *Kisseleviella* sp. A is the dominant diatom in most samples, accounting for more than 50% of the flora in some samples. The LO of *Kisseleviella* sp. A is abrupt and marks a significant unconformity near 130 mbsf.

Cymatosira sp. A Partial Range Zone, lower Miocene (this report)

Top: LO of *Cymatosira* sp. A 96.70 mbsf.

Bottom: LO of *Kisseleviella* sp. A, 130.90 mbsf.

The *Cymatosira* sp. A Zone is defined as the stratigraphic interval from the LO of *Kisseleviella* sp. A up to the FO of *Cymatosira* sp. A. Diatom preservation is good to moderate in the middle portion of this zone (Fig. 1). Several ash beds are noted in this zone, which contain very well-preserved diatom assemblages.

Rhizosolenia sp. B Interval Zone, lower Miocene (this report)

Top: FO of *Fragilariopsis* sp. A, 57.42 mbsf.

Bottom: LO of *Cymatosira* sp. A, 96.70 mbsf.

The *Rhizosolenia* sp. B Zone is defined as the stratigraphic interval from the LO of *Cymatosira* sp. A up to the FO of *Fragilariopsis* sp. A. The distinctive silicoflagellate *Septamesocena pappii* occurs throughout this zone, as well as the FO of *Dactyliosolen antarcticus*. The sample at 75.52-56 mbsf is notable in that it contains abundant *Rhizosolenia* spp., including *Rhizosolenia* sp. A and *Rhizosolenia* sp. B.

Fragilariopsis sp. A Partial Range Zone, lower Miocene (this report)

Top: FO of *Thalassiosira praefraga*, 36.25 mbsf.

Bottom: FO of *Fragilariopsis* sp. A, 57.42 mbsf.

The *Fragilariopsis* sp. A Partial Range Zone is defined as the stratigraphical interval from the FO of *Fragilariopsis* sp. A up to the FO of *Thalassiosira praefraga*. In CRP-2/2A, this zone comprises an interval of poor to moderate diatom preservation and relatively low diatom abundance (Fig. 1). This zone was not identified in the CRP-1 drillcore due to the coincident FO of *Thalassiosira fraga* and *Fragilariopsis* sp. A at the base of the *T. fraga* Zone (Harwood et al., 1998). This relationship suggests that the lower range of *Fragilariopsis* sp. A was truncated

in the CRP-1 drillcore. The occurrence of *Fragilariopsis* sp. A in CRP-2/2A may represent the lowest (oldest) known occurrence of the genus *Fragilariopsis*, which today dominates the Antarctic sea-ice zone.

Thalassiosira praefraga Range Zone, lower Miocene (Harwood et al., 1998)

Top: LO of *Thalassiosira praefraga*, unconformity at c. 28 mbsf.

Bottom: FO of *Thalassiosira praefraga*, 36.25 mbsf.

The *Thalassiosira praefraga* Range Zone is defined as the interval including the stratigraphic range of *T. praefraga*. The upper range of *T. praefraga* is not complete in CRP-2/2A due to an unconformity at c. 28 mbsf, which separates lower Miocene from Plio-Pleistocene strata. Diatoms in the *Thalassiosira praefraga* Zone of CRP-2/2A are moderately preserved with a moderately diverse diatom assemblage including *T. praefraga*, *Fragilariopsis* sp. A, *Thalassiosira nansenii*, *Dactyliosolen antarcticus*, and "Tigeria" spp.

DISCUSSION

AGE AND STRATIGRAPHICAL CORRELATIONS

Diatoms are the primary fossil group providing biostratigraphical age control for the CRP-2/2A drillcore. Assemblages from the lower Oligocene to lower Miocene section of CRP-2/2A are predominantly neritic-planktic in character, and open-ocean diatom taxa that are common in Southern Ocean drillcores are rare or absent. However, several diatom events with known age calibration are recognised (Tab. 4). Age calibration of these datums is based on correlation with the magnetostratigraphical records of ODP legs 120 (Harwood & Maruyama, 1992), 119 (Baldauf & Barron, 1991), and several North Pacific cores (Yanagisawa & Akiba, 1998).

Previous drillcores in McMurdo Sound offer useful constraint on biostratigraphic ranges and the stratigraphic sequence of specific diatom taxa. These cores include MSSTS-1 drillcore (Harwood, 1986), CIROS-1 drillcore (Harwood, 1989), CRP-1 drillcore (Harwood et al., 1998) and CRP-3 drillcore (Cape Roberts Science Team, 2000). Occurrence data of key taxa in these McMurdo Sound drill-cores are presented in table 4, and a proposed correlation scheme between CRP-2/2A, and CIROS-1, based on diatom distributions, is shown on figure 3. The stratigraphic distribution of diatoms in the CRP-2/2A drillcore provides a framework for correlating these earlier drillcores, though stratigraphic overlap is minimal.

The FO of common *Thalassiosira praefraga* provides a primary correlation point between the CRP-1 (Roberts et al., 1998) and CRP-2/2A drillcores (Wilson et al., this volume). This datum occurs at 103.39 mbsf in CRP-1 and at 36.24 mbsf in CRP-2/2A. Based on magnetostratigraphical correlations for each hole, this datum occurs in the lower portion of Chron C5En at c. 18.7 Ma (Roberts et al., 1998; Wilson et al., this volume). This indicates a

Tab. 4 - Deep-sea ranges of selected Oligocene-early Miocene diatom taxa and occurrence in CRP-2/2A and other McMurdo Sound drillcores.¹

Species	Datum	Age Range (Ma / Chron)	Occurrence in CRP-2/2A (mbsf)	Occurrence in McMurdo Sound Cores (mbsf)	Sources
<i>Thalassiosira praefraga</i>	D1 (FO)	20.3 ^t (FCAD) to 18.3 ^t (C6r to C5En)	FO at 36.25	FO at 103.39 (CRP-1)	H&M / Y&A / H*
<i>Cavitätus rectus</i>	-	LO at ~20.5 ^t (C6r)	Not present	LO at 146.79 (CRP-1)	A+ / Y&A
<i>Dactyliosolen antarcticus</i>	-	26.5 ^s to present (C8n,2n)	FO at 75.56	Ranges through lower Miocene of CRP-1	H&M / H*
<i>Lisitzinia ornata</i>	D2 (LO)	28.3 ^s to 24.1 ^s (C9r to C6Cr)	266.38 to 259.21	Not present in CRP-1 309.38 (CIROS-1) 222.04 to 187.21 (MSSTS-1)	H / H* / B / H&M
<i>Eurossia irregularis</i> (syn. <i>Triceratium hebetatum</i>)	D3 (LO)	>27-29 (C9-C10)	564.66 to 412.27	500.14 to 371.06	H* / H&M
<i>Asteromphalus symmetricus</i>	-	28.7 ^s to 18.3 ^s (C10n,2n to C5En)	Lowest confirmed occurrence at 236.25	LO at 84.00 (CRP-1) 179.32 to 149.26 (CIROS-1) 222.58 to 61.52 (MSSTS-1)	H / H* / H&M / H+
<i>Asterolampra punctifera</i>	D4 (LO)	LO at 27.0 ^s (C9n)	Highest confirmed occurrence at 444.96	500.14 to 382.70 (CIROS-1)	H* / H&M
<i>Rhizosolenia oligocaenica</i>	D5 (LO)	LO at 29.6 ^s (C11n,1r)	483.93 to 444.96	428.00 to 382.70 (CIROS-1)	H* / H&M
<i>Pyxilla reticulata</i>	D6 (LO)	LO at 30.1 ^s (C11r)	Fragments occur up to 309.88	661.13 to 366.99 (CIROS-1)	H* / H&M
<i>Cavitätus jouseanus</i>	D7 (FO)	30.9 ^s to 14.6 ^s (C12n to C5ADr)	543.81 to 28.90	147.69 to 99.02 (CRP-1) 359.63 to 110.26 (CIROS-1) 222.58 to 50.88 (MSSTS-1)	H / H* / B / H&M / Y&A / H+
Assemblage B (CIROS-1)	D8 (LO)	~33.0 (C13n)	Not recorded in CRP-2/2A (>564.67)	>366.99 (CIROS-1)	H*

¹Ages are calibrated to the Berggren et al. (1995) time scale. Ages indicated with § are datums derived from Southern Ocean cores, and those indicated with † are datums derived from North Pacific cores. Information is compiled from the following sources: H = Harwood (1986), H* = Harwood (1989), B = Baldauf & Barron (1991), H&M = Harwood & Maruyama (1992), A+ = Akiba *et al.* (1993), Y&A = Yanagisawa & Akiba (1998), and H+ = Harwood *et al.* (1998).

younger age for this datum than that applied from the North Pacific region, where this datum occurs at 20.3 Ma, in Chron C6r (Yanagisawa & Akiba, 1998).

The top of the *Cavitätus rectus* Zone is noted in CRP-1 at 147.48 mbsf (Harwood *et al.*, 1998), but it is not recognised in CRP-2/2A. This may be due to a stratigraphic gap between 65 to 70 mbsf, or that this rare taxon was simply not encountered in examination of the CRP-2/2A drillcore.

The Miocene/Oligocene boundary is present in CRP-2/2A at ~180 mbsf (Wilson *et al.*, this volume) within the *Kisseleviella* sp. A Zone. A significant change in the diatom assemblage is recognised ~50 m above this level at 130.90 mbsf, which appears to mark a significant disconformity. *Kisseleviella* sp. A is common in assemblages below 130.90 mbsf and absent from assemblages above that unconformity, marking the LO of this taxon. *Kisseleviella* sp. A occurs in MSSTS-1 from the base of that core at 222.58 mbsf to 50.88 mbsf (Harwood, 1986), and in CIROS-1 from c. 366 to 145.15 mbsf (Harwood, 1989). The LO of this taxon in CIROS-1 and in CRP-2/2A provides a point of correlation between these drillcores (Fig. 3), although it is most likely truncated at a disconformity in each drillcore.

Kisseleviella sp. A is an undescribed taxon which occurs in CRP-2/2A, MSSTS-1, and CIROS-1. Illustrated specimens, designated as *Kisseleviella carina* by Harwood (1986, p. 86, pl. 6, figs. 12-15) from several intervals in the MSSTS-1 drillcore are similar in rhombic-lanceolate form as those designated as *Kisseleviella* sp. A in this report, but

Kisseleviella sp. A is taxonomically distinct from *Kisseleviella carina* (Sheshukova-Poretskaya, 1962) *sensu stricto*. A reexamination of CIROS-1 samples shows that the *Kisseleviella* species above the unconformity at c. 366 mbsf in CIROS-1 is of *Kisseleviella* sp. A (of CRP-2/2A), whereas *Kisseleviella* sp. G (this report) and related forms occur below the unconformity in CIROS-1. None of the *Kisseleviella* species reported as *K. carina* in Southern Ocean sediments (Hajós, 1976, pl. 25, figs. 5-9, & 14; Harwood, 1989, pl. 4, fig. 36; Barron & Mahood, 1993, pl. 5, fig. 11), conform to the description and type illustrations of *Kisseleviella carina* Sheshukova-Poretskaya from the Miocene of the North Pacific region (see additional notes in systematic palaeontology section).

The uppermost interval of the *Hemiaulus* sp. A Zone and the lowermost interval of the *Pterotheca reticulata* Zone in CRP-2A (~265 to 255 mbsf) are interpreted to represent a strong pulse of biosiliceous sedimentation on the Antarctic continental shelf (Tab. 1; Fig. 1). The LO of *Lisitzinia ornata* occurs within this interval. *Lisitzinia ornata* ranges from Chrons C9r to C6r (28.3 to 24.2 Ma) in the Southern Ocean (revised ages from Harwood and Maruyama, 1992). *Lisitzinia ornata* is a pelagic species that is probably excluded ecologically from the Antarctic continental shelf, except during intervals of enhanced exchange with pelagic water masses. Consequently, the range of *L. ornata* in CRP-2/2A most likely represents only a part of the total range of this taxon in the deep sea. This taxon is reported from one sample in CIROS-1 at 309.38 mbsf (Harwood, 1989) and between 222.58 and

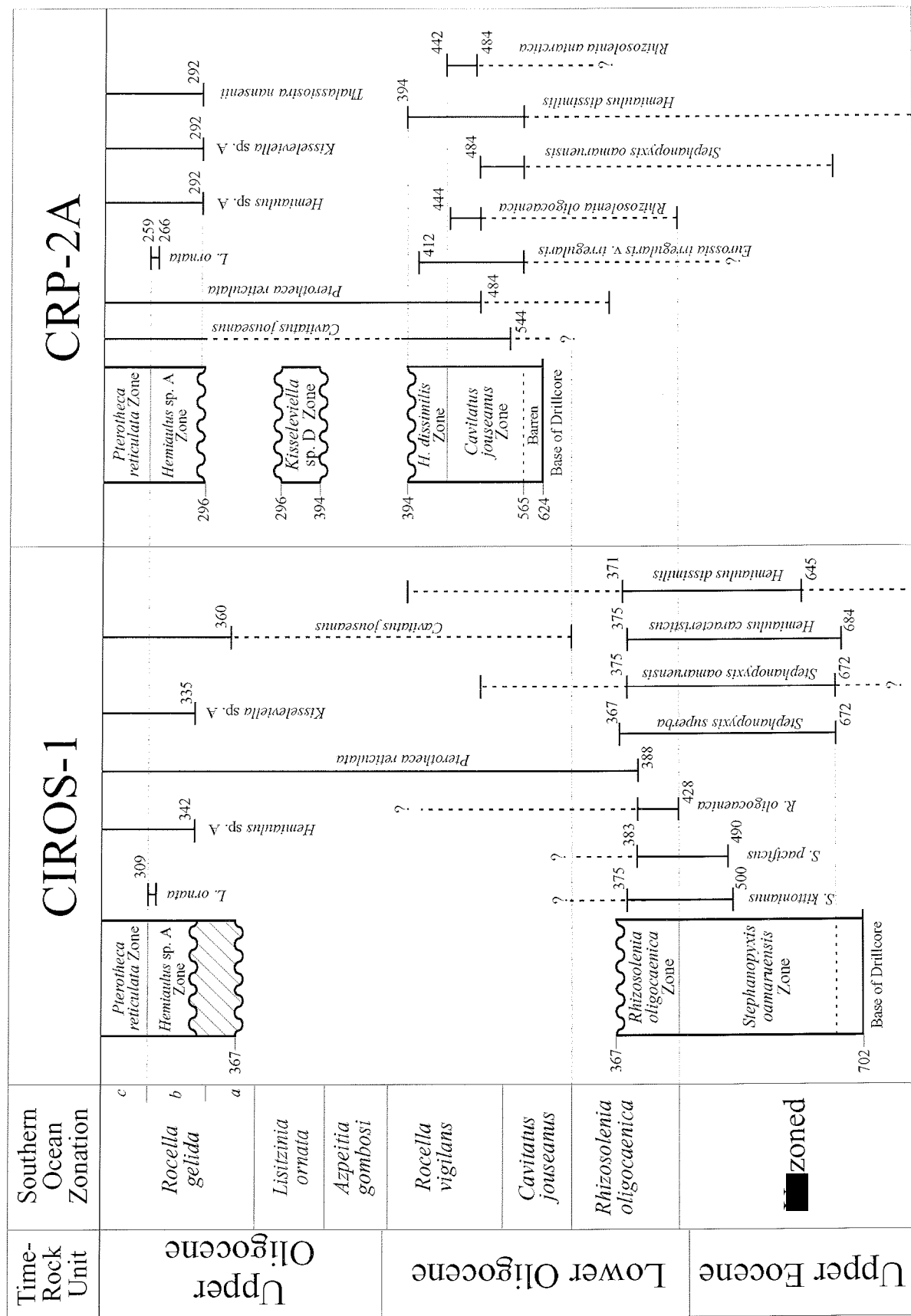


Fig. 3 - Proposed correlation of CRP-2A with CIROS-1 based on diatoms. This correlation suggests that much of CRP-2A, from the base of the hole at 624 mbsf up to c. 300 mbsf is not represented in CIROS-1. Stratigraphical ranges and depths of key diatoms are presented for each core

122.87 mbsf in the MSSTS-1 drillcore (Harwood, 1986). These occurrences may represent a correlative interval to the *L. ornata* occurrences noted in CRP-2/2A (Fig. 3).

The datums defining the *Hemiaulus* sp. A Zone are not calibrated to the magnetic polarity time scale. The FO of *Hemiaulus* sp. A (at 296.41 mbsf) is truncated at an interval of poor preservation from 412.27 to 296.41 mbsf. $^{40}\text{Ar}/^{39}\text{Ar}$ ages indicate an age of 24.22 Ma at c. 280 mbsf and a maximum age of 24.98 Ma at 294.22 mbsf for this interval (McIntosh, this volume) (Fig. 2), placing the *Hemiaulus* sp. A Zone in the upper part of the upper Oligocene. The *Hemiaulus* sp. A Zone is correlative with portions of the Southern Ocean *Rocella gelida* Zone. We presume that *R. gelida* is excluded or reduced ecologically from the Antarctic neritic region represented in CRP-2/2A.

The *Kisseleviella* sp. D Interval Zone (from 394.48 to 296.41 mbsf) is an interval containing poorly-preserved diatoms in low abundance. Many samples within this interval are barren of diatoms (Fig. 1). Diatom biostratigraphic age assessment of this zone, therefore, is difficult, but the occurrence of rare specimens of *Pyxilla* spp. indicates a lower Oligocene position. Fragments and rare specimens of *Pyxilla* spp. may have been reworked, however, and this interpretation is presented with some uncertainty.

The *Hemiaulus dissimilis* Zone, which is recognised between 441.85 and 394.48 mbsf, is assigned a stratigraphical position in the lower upper Oligocene, based diatom biostratigraphy. The occurrence of *Eurossia irregularis* var. *irregularis*, *Hemiaulus dissimilis*, and *Pyxilla* spp. in this interval suggests a stratigraphical position of lower Oligocene. *Eurossia irregularis* and *Hemiaulus dissimilis* have not been reported in upper Oligocene sediments in the Southern Ocean or from other McMurdo Sound drillcores, but they are rare in deep-sea sediments, and their ranges have not been well-documented or previously calibrated on the continental shelf.

The *Cavittatus jouseanus* Zone is the lowest zone noted in the CRP-2/2A drillcore. The lowest specimen of *C. jouseanus*, which defines the base of this zone, is noted at 543.81 mbsf, but this is truncated below by an interval of poor preservation (Fig. 1). The *C. jouseanus* Zone continues below the base of the CRP-2/2A, as this taxon occurs to a depth of 44.83 mbsf in the CRP-3 drillcore. The FO of *S. jouseanus* is difficult to identify, as this taxon is rare in its early range (Fenner, 1984). This datum is calibrated with Chron C12n at 30.9 Ma (Harwood & Maruyama, 1992, adjusted age). Early specimens of *C. jouseanus* noted in the lower portion of the range are smaller and more slender than typical specimens of this taxon.

Rhizosolenia oligocaenica, which occurs in CRP-2/2A from 483.92 to 443.89 mbsf, ranges in the Southern Ocean from 33.6 to 29.6 Ma, within Chrons C13n to C11n.1r. Occurrences of this taxon as young as 29.6 Ma, were considered previously to be reworked (Harwood & Maruyama, 1992). However, in light of multiple Sr ages in the range 29.89 Ma to 29.41 Ma (Lavelle, this volume) from sediments containing *R. oligocaenica* in CRP-2/2A, it appears as though the Southern Ocean occurrences at 29.6 Ma (Site 748B) could be *in situ*. This results in the extension of the upper range of *R. oligocaenica* to c. 29.6

Ma in the high southern latitudes.

The lowest three diatom zones in CRP-2A (below 296.41 mbsf) are interpreted represent part of the stratigraphical section missing in the unconformity in the CIROS-1 drillcore at c. 366 mbsf (Fig. 3). Key taxa present below c. 366 mbsf in CIROS-1, such as *Archaeosphaeridium australensis*, *Ebrinula paradoxa*, *Hemiaulus characteristicus*, *Stephanopyxis splendidus*, and common *Stephanopyxis superba*, are not present in CRP-2/2A (Tab. 5). This suggests the lower part of CRP-2A is confined to a higher stratigraphic interval than represented by sediments below the unconformity is CIROS-1. The interval just below c. 366 mbsf in CIROS-1 is assigned an earliest Oligocene age of c. 33 Ma (Wilson et al., 1998). This age assignment supports an early Oligocene age of the oldest sediments recovered in CRP-2/2A.

DIATOM PALAEOENVIRONMENTS

The diatom record of CRP-2/2A is strongly dominated by planktic diatoms associated with the neritic environments, such as *Stephanopyxis* spp. Benthic taxa are rare

Tab. 5 - Siliceous microfossil taxa with ranges restricted to intervals below the unconformity (at ~366 mbsf) in CIROS-1¹.

<i>Archaeosphaeridium australensis</i> *
<i>Archaeosphaeridium tasmaniae</i>
<i>Asterolampra punctifera</i>
<i>Dictyocha deflandrei</i>
<i>Ebrinula paradoxa</i> *
<i>Ebriopsis crenulata</i> (loricate)*
<i>Ebriopsis crenulata</i> *
<i>Eurossia irregularis</i> v. <i>irregularis</i>
<i>Hemiaulus characteristicus</i> *
<i>Hemiaulus dissimilis</i>
<i>Kanno hastata</i> ²
<i>Kisseleviella</i> sp. G (= <i>K. carina</i> sensu Harwood, 1989, in part) ³
<i>Parebriopsis fallax</i> *
<i>Pseudammochidium dictyoides</i> *
<i>Ptherotheca danica</i> *
<i>Pyxidicula</i> sp. A*
<i>Pyxilla eocena</i>
<i>Pyxilla reticulata</i>
<i>Rhizosolenia oligocaenica</i>
<i>Rouxia granda</i>
<i>Sceptroneis lingulatus</i>
" <i>Skeletonema</i> " <i>utriculosa</i> ⁴ *
<i>Sphinctolethus pacificus</i> *
<i>Stephanopyxis oamaruensis</i>
<i>Stephanopyxis superba</i> *
<i>Stictodiscus kittonianus</i> *
<i>Vulcanella hanna</i>

¹Taxa indicated with an asterisk were not observed in CRP-2/2A.
Siliceous microfossil ranges from CIROS-1 are reported in Harwood (1989) and Bohaty & Harwood (2000).

²Identified as *Ikebea tenuis* in the CIROS-1 drillcore (Harwood, 1989).

³*Kisseleviella* specimens below 366 mbsf in CIROS-1 (designated as *Kisseleviella carina* by Harwood (1989)) may represent a new species, taxonomically separate from *Kisseleviella carina* Sheshukova-Poretskaya.

⁴Identified as *Paralia oamaruensis* in the CIROS-1 drillcore (Harwood, 1989).

throughout most intervals of CRP-2/2A. Diatom assemblages from 110 to 114 mbsf (within a zone containing several volcanic ash horizons), however, include the large and distinctive benthic diatom taxon, "Genus and species uncertain A," reported from the lower Miocene section of CRP-1 (Harwood et al., 1998). Otherwise, *Cocconeis* spp., *Rhabdonema* spp., *Arachnoidiscus* spp., and fragments of large *Isthmia* sp. are noted throughout the CRP-2/2A section, but in low abundance (0-5%). These are interpreted as likely allochthonous and derived from an adjacent shallow-coastal environment. Furthermore, the low relative abundance of benthic diatom taxa suggests water-depths below the photic zone (>50m water depth) for most of the interval recovered in CRP-2/2A. Light penetration, however, may have been limited due to water turbidity from high input of glacially-derived sediment, which may have suppressed growth of a benthic flora. This possibility is also supported by high sediment accumulation rates that are interpreted for most of the CRP-2/2A section, based on the biostratigraphically- and geochronologically-constrained age model (Wilson et al., this volume).

The low abundance of benthic diatoms in CRP-2/2A contrasts with assemblages documented in the CRP-1 and CIROS-1 drillcores, which include intervals with significant concentrations of benthic diatoms (Harwood, 1989; Harwood et al., 1998). Benthic diatom assemblages from 59.99 to 58.05 mbsf in Lithostratigraphic Unit 5.2 of CRP-1, for example, indicate shallow deposition in water-depths 50 m or less (Harwood et al., 1998). These data suggest deeper overall palaeo-water depths for CRP-2/2A than was interpreted for either the CIROS-1 or CRP-1 drillcore.

Several intervals of high abundance of planktic diatoms are noted in CRP-2/2A (Fig. 1). High diatom abundance commonly corresponds with intervals of finer-grained facies, with the exception of intervals that have undergone significant diagenesis. Intervals of high diatom accumulation are interpreted to indicate open water and high nutrient availability. Common to abundant diatoms are closely associated with the fined-grained, mudstone facies of Lithostratigraphic units 13.1, 9.7, and 8.4, which are interpreted as "highstand systems tract" intervals of depositional sequences 19, 11, and 9, respectively (Cape Roberts Science Team, 1999). The interval of highest diatom abundance (Fig. 1) in CRP-2/2A occurs between 263.21 and 254.43 mbsf; fossiliferous mudstone of Unit 9.7 (262.90 to 250.40 mbsf). Planktic siliceous microfossils in this interval comprise a significant percentage of the clay and silt-sized fraction, and are interpreted to indicate highly productive open waters with bottom depths most likely exceeding 100 m. The occurrence of several open-marine taxa, such as *Lisitzinia ornata* in this interval, indicate an event of pelagic sedimentation. Common to abundant diatoms are also present from 474.90 to 446.55 mbsf, including most of Unit 13.1 (468.00 to 442.99 mbsf), from 181.33 to 176.29 mbsf, representing an interval within Unit 8.4 (183.35 to 153.39 mbsf), and from 138.84 to 130.90 mbsf, representing Unit 8.2.

Diatoms are common and well-preserved in association with ash and lapillistone in Unit 7.2 (109.07 to 114.21

mbsf). The occurrence of glassy ash in sediments commonly acts to buffer pore waters with silica, enhancing potential for diatom preservation. Well-preserved diatom assemblages in CRP-2/2A are also commonly associated with intervals containing well-preserved macrofossils.

Several intervals barren of diatoms (or only trace occurrences) are noted in CRP-2/2A (Fig. 1) and are interpreted to indicate ice cover, extremely high sedimentation rate, diagenetic dissolution of biogenic opal, or a combination of these factors. The interval from 412.27 to 292.08 mbsf is largely barren of diatoms. Dinoflagellate assemblages are present throughout this interval (Cape Roberts Science Team, 1999), suggesting that diagenetic effects, rather than environmental exclusion, are at least partially responsible for the absence of diatoms. With the exception of rare, recrystallized forms, diatoms are also absent from 564.66 mbsf to the base of the hole at 624.15 mbsf, an interval which may have similarly been affected by diagenesis.

Diatoms provide little direct information regarding surface-water palaeotemperatures through the lower Oligocene to lower Miocene section of CRP-2/2A; most taxa are extinct, and their palaeobiogeographic distributions during the Paleogene are unknown. Furthermore, diatoms provide no unequivocal evidence for the presence or absence of sea-ice. The first occurrence of the genus *Fragilariopsis* Hasle, however, in the lower Miocene of CRP-1 and CRP-2 could possibly mark a significant environmental change in the marginal seas surrounding Antarctica. Members of this genus dominate the modern sea-ice habitat (most notably *Fragilariopsis curta* and *F. cylindrus*) and share significant morphologic features with the lower Miocene *Fragilariopsis* sp. A.

Specimens of the Parmales, a group of siliceous nannoplankton, were also observed, down to at least 292.28 mbsf. The presence of Parmales may similarly indicate the presence of sea-ice, based on high relative abundance in surface sediments of the southern Weddell Sea (Zielinski, 1997). We acknowledge that palaeoecological interpretations such as these are speculative.

SUMMARY

The CRP-2/2A drillcore provides a detailed stratigraphical record for the Antarctic continental shelf, despite numerous disconformities and at least 3 major unconformities. The age model for CRP-2/2A (Wilson et al., this volume) suggests high sediment accumulation rates throughout the recovered successions, especially between c. 80 and c. 300 mbsf. Several distinct neritic diatom assemblages are identified through the core, and numerous FO and LO datums provide a basis for a detailed diatom biostratigraphical zonation. From diatom biostratigraphy, the interval from 25.92 mbsf to 130.27 mbsf is interpreted to be lower Miocene; the interval from 130.27 to 296.41 mbsf to be upper Oligocene; and the interval from 394.48 mbsf to the bottom of the hole to be lower Oligocene. The interval from 296.41 to 394.48 is most likely lower Oligocene, but this assignment is

equivocal due to poorly-preserved diatom assemblages.

Application of diatom biostratigraphy as a tool for Miocene and Oligocene age control on the Antarctic continental shelf is currently dependent on the recognition of Southern Ocean zonal taxa that are calibrated to the magnetic polarity time scale. This dependence is due to the lack of any other reference holes on the continental shelf. The documentation and calibration of diatom biostratigraphic events based on the more abundant and persistent taxa in the CRP drillcores will enable significant improvement in biostratigraphic age control on the continental shelf. Future drilling on the Antarctic shelf will not rely on the application of rare Southern Ocean taxa, but will be able to apply the zonation developed herein for the lower Miocene to lower Oligocene.

TAXONOMIC LIST AND RELEVANT SYSTEMATIC PALAEONTOLOGY

The following is a listing of taxa or taxonomic groups encountered in this study. Rare taxa and those with sporadic occurrences are listed below with brief occurrence data and not included on table 2. Many diatoms are reported only to genus level and many taxa are reported under informal names. Informal taxonomy presented here reflects the “work-in-progress” state of the Cape Roberts Project diatom studies. We do not include detailed reference to these taxa as the reader should refer to the works of Harwood (1986), Harwood (1989), Harwood et al. (1989a), Harwood & Maruyama (1992), Barron & Mahood (1993), Mahood et al. (1993) for synonymy. Where necessary, we cross reference to species names used in the above papers, if names or taxonomic concepts have changed recently.

DIATOMS

***Achnanthes* spp.** Comments: Sparse occurrences of this genus are noted between 96 and 271 mbsf.

Actinoptychus senarius (Ehrenberg)

Arachnoidiscus cf. sendaiicus Brown, 1933, p. 57, pl. 1, fig. 1, pl. 4, figs. 6-8; Hanna et al., 1976, p. 11, pl. 2, fig. 6; *Arachnoidiscus* sp. A of Harwood, 1986, p. 85, pl. 1, figs. 4-5. (Pl. 6, Fig. 2)

***Arachnoidiscus* spp.** Comments: Rare specimens of *Arachnoidiscus* were noted in many CRP-2/2A samples, commonly as fragments in unsieved material (Pl. 6, Fig. 2).

Asterolampra punctifera (Grove) Hanna. (Pl. 6, Fig. 1)

Asteromphalus symmetricus Schrader & Fenner.

Asteromphalus* sp. cf. *A. symmetricus Schrader & Fenner of Harwood et al., 1989a, pl. 4, fig. 3.

***Asteromphalus* sp. A.** Comments: An unknown morphology of *Asteromphalus* occurs at 71.13-14 mbsf, referred to here as *Asteromphalus* sp. A. This form is similar to the diatom identified as *Asteromphalus hyalinus* Karsten in Harwood, 1986, pl. 1, fig. 7, (originally thought to be a downhole contaminant), and *Asteromphalus inaequabilis* Gersonde in Harwood & Maruyama, 1992, pl. 5, figs. 1, 2. (Pl. 5, Fig. 5)

Aulacodiscus browniei Norman sensu McCollum, 1975,

and Harwood et al., 1989a.

Azpeitia oligocaenica (Jousé) Sims. Comments: Rare specimens and fragments of this taxon occur between 130.90 and 122.56 mbsf.

Cavitatus jouseanus (Sheshukova-Poretskaya) Williams; Akiba et al., 1993, p. 20-22, fig. 6-19, 6-20. Comments: Specimens of *Cavitatus jouseanus* present in CRP-2/2A differ from *C. jouseanus* s.s. in that they tend to be smaller and more lightly silicified with narrow, tapered ends (rather than broadly-rounded ends). This is particularly true in the lower range of its occurrence in CRP-2/2A, below 444 mbsf. Fragmented or broken specimens of *Cavitatus jouseanus* were difficult to distinguish from *C. miocenicus*, or other *Cavitatus* taxa. Occurrences documented in this report, however, are based on complete or nearly complete, identifiable valves.

Cavitatus miocenicus (Schrader) Akiba & Yanagisawa in Akiba.

Chaetoceros panduraeformis (Pantocsek) Gombos (Pl. 5, Fig. 11).

***Chaetoceros* spp.** and related spore-forming genera.

Comments: Many distinct morphotypes of *Chaetoceros* are recognised, but are combined for this report. Group A includes simple Hyalocheate spores and vegetative cells of the variety abundant in modern Antarctic sediments (see Harwood, 1986, pl. 7, figs. 1-12). Group B includes larger spores with large bifurcate setae such as illustrated by Harwood, 1986, pl. 3, figs. 1-4; Harwood et al., 1989a, Pl. 3, Fig. 4. This morphotype is no longer present in Antarctic coastal waters. Group C is an informal grouping of numerous relatively large and heavily-silicified spore “genera,” including *Chaetoceros*-like resting-spores referred to as *Liradiscus* Greville, *Chasea* Hanna, and *Xanthiopyxis* Ehrenberg, among others.

***Coccconeis* spp.**

Coscinodiscus* sp. cf. *C. marginatus Ehrenberg (Pl. 5, Fig. 7).

Corethron criophilum Castracane. Comments: *Corethron criophilum* is present in one sample at 271.02 mbsf.

***Coscinodiscus* spp.** Comments: This group includes many large *Coscinodiscus* species, which are generally present as fragments in unsieved samples.

Cymatosira praecompacta Schrader and Fenner.

***Cymatosira* sp. A.** Description and Comments: This species has a broad, sub-circular valve shape, with narrow, sharply tapering to apiculate apices. Areolae are arranged in broad and disorganized, transapical rows across the valve face. This diatom has been referred to as *Cymatosira biharensis* by Fenner (1985, figs. 7.19-22). (Pl. 2, Figs. 18-19)

Dactyliosolen antarcticus Castracane. Harwood & Maruyama, 1992, p. 702, pl. 18, fig. 12.

***Diploneis* spp.**

Distephanosira architecturalis (Brun) Gleser et al. Comments: Very rare examples of small-diameter *Distephanosira architecturalis* occur in lower Oligocene samples of CRP-2/2A. Small specimens are characteristic of the highest range of this taxon, unlike large specimens typical of Eocene sediments.

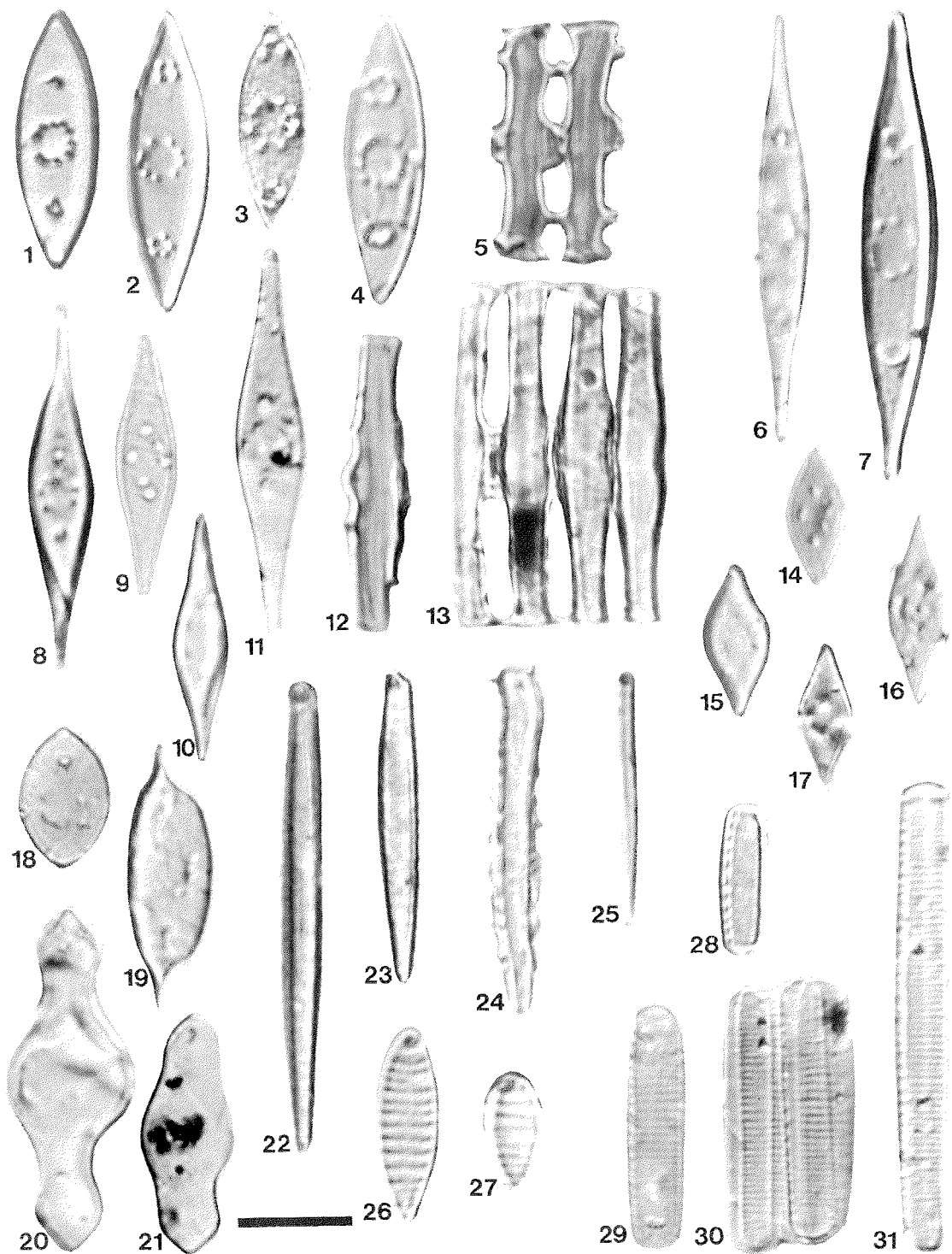


Plate 1 - Scale bar equals 10µm; all are valve views unless indicated otherwise.

Figures 1-5. *Kiszeleviella* sp. A; (1) CRP-2/2A-271.02-.04 m; (2) CRP-2/2A-210.58-.59 m; (3) CRP-2/2A-271.02-.04 m; (4) CRP-2/2A-195.70-.72 m; (5) Girdle view, CRP-2/2A-264.38-.39 m.

Figures 6-7. *Kiszeleviella* sp. B; (6) CRP-2/2A-292.08-.10 m; (7) CRP-2/2A-271.02-.04 m.

Figures 8-13. *Kiszeleviella* sp. C; (8) CRP-2/2A-474.90-.91 m; (9) CRP-2/2A-474.90-.91 m; (10) CRP-2/2A-464.98-.00 m; (11) CRP-2/2A-474.90-.91 m; (12) Girdle view, CRP-2/2A-474.90-.91 m; (13) Girdle view, CRP-2/2A-483.92-.93 m.

Figures 14-17. *Kiszeleviella* sp. D; (14) CRP-2/2A-474.90-.91 m; (15) CRP-2/2A-464.98-.00 m; (16) CRP-2/2A-474.90-.91 m; (17) CRP-2/2A-464.98-.00 m.

Figure 18. *Kiszeleviella* sp. E; CRP-2/2A-282.42-.43 m.

Figure 19. *Kiszeleviella* sp. F; CRP-2/2A-543.81-.83 m.

Figures 20-21. *Kiszeleviella* sp. G; (20) CRP-2/2A-474.90-.91 m; (21) CRP-2/2A-474.90-.91 m.

Figures 22-23. *Ikebea* sp. B; (22) CRP-2/2A-271.02-.04 m; (23) CRP-2/2A-271.02-.04 m.

Figure 24. *Ikebea* sp. C; CRP-2/2A-236.25-.26 m.

Figure 25. *Ikebea* sp. A; CRP-2/2A-444.96-.98 m.

Figures 26-27. *Kanno hastata* Komura; (26) CRP-2/2A-443.89-.90 m; (27) CRP-2/2A-464.98-.00 m.

Figures 28-31. *Fragilariopsis* sp. A of Harwood et al. (1998); (28) CRP1-99.02-.25 m; (29) CRP1-99.02-.25 m; (30) CRP1-99.02-.25 m; (31) CRP1-99.02-.25 m.

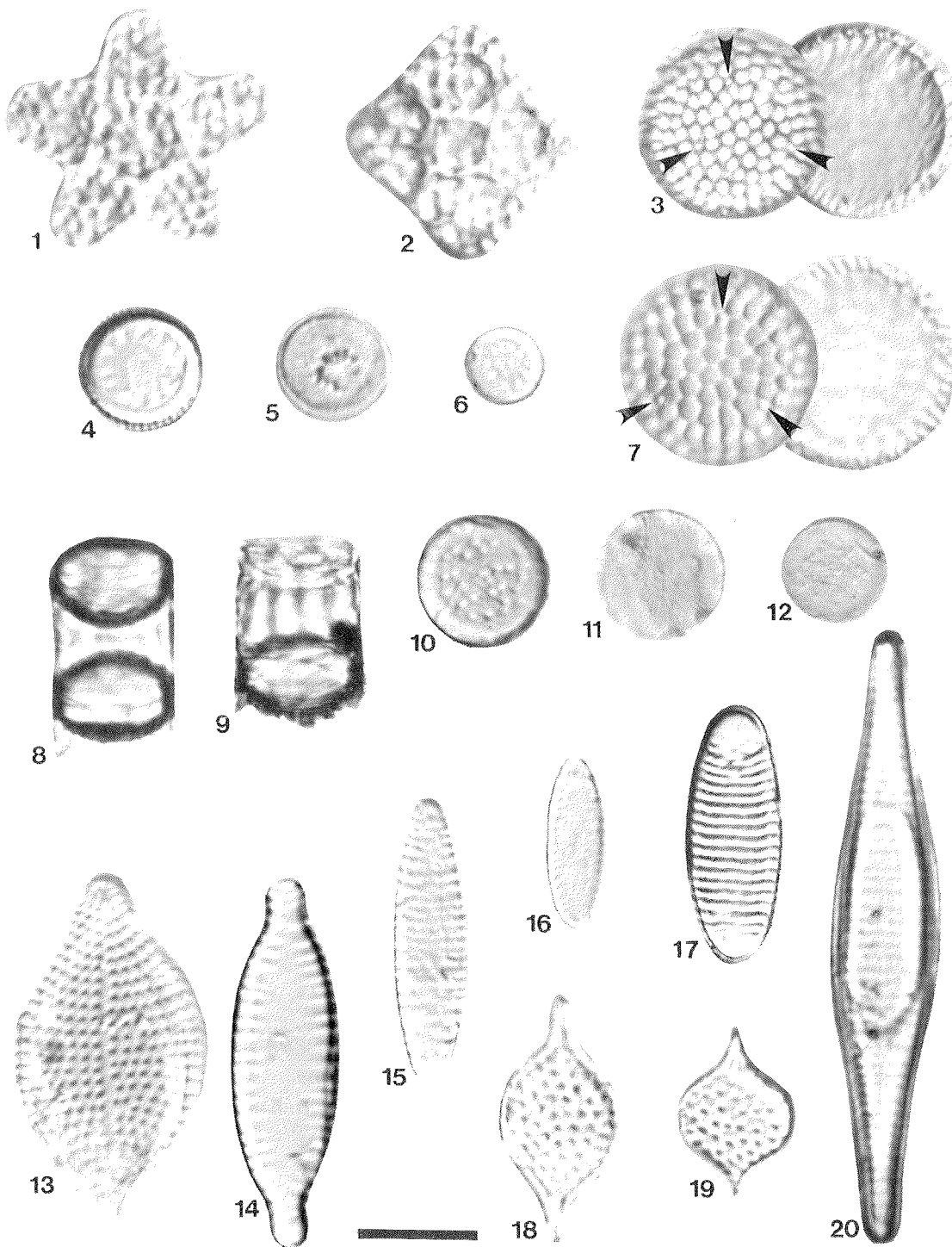


Plate 2 - Scale bar equals 10 μ m; all are valve views unless indicated otherwise.

Figure 1. *Lisitzinia ornata* f. *pentagona* Harwood; CRP-2/2A-263.20-.21 m.

Figure 2. *Lisitzinia ornata* Jousé; CRP-2/2A-264.38-.39 m.

Figures 3, 7. *Thalassiosira praefraga* Gladenkov & Barron; (3) CRP2-36.24-.25 m; (7) CRP2-36.24-.25 m (arrows denote positions of strutted processes).

Figures 4-6. *Trochosira spinosus* Kitton; (4) CRP-2/2A-264.38-.39 m; (5) CRP-2/2A-271.02-.04 m; (6) CRP-2/2A-264.38-.39 m.

Figures 8-12. *Skeletonemopsis mahoodii* Sims; (8) Girdle view of two frustules, CRP-2/2A-542.04-.05 m; (9) Girdle view, CRP-2/2A-542.04-.05 m; (10) CRP-2/2A-464.98-.00 m; (11) CRP-2/2A-543.81-.83 m; (12) CRP-2/2A-474.90-.91 m.

Figure 13. *Rhaphoneis amphiceros* (Ehrenberg) Ehrenberg; CRP-2/2A-264.38-.39 m.

Figure 14. "Tigeria" sp. A; CRP-2/2A-75.52-.56 m.

Figure 15. "Tigeria" sp. B; CRP-2/2A-75.52-.56 m.

Figure 16. "Tigeria" sp. C; CRP-2/2A-271.02-.04 m.

Figures 17. *Rhabdonema* sp.; CRP-2/2A-271.02-.04 m.

Figures 18-19. *Cymatosira* sp. A; (18) CRP-2/2A-271.02-.04 m; (19) CRP-2/2A-271.02-.04 m.

Figure 20. *Grammatophora* sp.; CRP-2/2A-271.02-.04 m.

Endictya hungarica Hajós. Comments: This taxon is present between 483.92 and 464.98 mbsf.

Entopyla australis Ehrenberg. (Pl. 5, Fig. 10)

Eurossia irregularis* var. *irregularis (Greville) Sims, in Mahood et al., 1993, p. 254-255; *Triceratium hebetatum* (Grunow) sensu Harwood, 1989; *Triceratium polymorphum* Harwood and Maruyama 1992, pro parte. (Pl. 4, Figs. 7, 9)

Eurossia irregularis* var. *irregularis (centrally swollen valve). Comments and description: In the present study, a morphotype that is structurally different from *Eurossia irregularis* var. *irregularis* was observed both individually and paired with specimens of normal wall structure. The morphology of the centrally swollen valves are triangular and thick-walled, with a raised, swollen valve center; areolae are small, 5 - 6 in 10 μ m, and inter-areolar architecture is thick with an echinate texture. Distinguishing processes at valve apices were not observed in LM examination. This morphology of *Eurossia irregularis* var. *irregularis* represents either a semi-endogenous resting spore valve or one valve of a heterovalve frustule. Neither resting spores nor heterovalve have been previously reported for this genus. Note however that *Pseudotriceratium alderi* Mahood in Mahood et al., 1993, is also heterovalvar; one valve possesses a centrally swollen region, the other valve is flat to concave. The feature noted here in *Eurossia irregularis* var *irregularis*, as well as the different structure of the apices suggests that *Pseudotriceratium alderi* belongs within the genus *Eurossia*. (Pl. 4, Figs. 1-2)

Extubocellulus spinifera (Hargraves & Guillard) Hasle et al., 1983. Comments: This small diatom (<4 μ m) has not been previously reported from the fossil record. Its small size and unusual shape make it easily overlooked or not recognized as a diatom. The specimens in CRP-2/2A closely resemble the description in Round et al. (1990).

***Fragilariopsis* sp. A** of Harwood et al., 1998; *Nitzschia* sp. A of Harwood et al., 1989a, p. 105, pl. 4, figs. 12-14; *Nitzschia truncata* Brady, 1979, 1980; *Nitzschia curta* sensu Kellogg & Kellogg, 1986, pl. 2 (not fig. 23). Description: Valves rectangular, valve face flat; forming ribbon-like colonies. Length, generally 12 - 20 μ m, with rare specimens in excess of 40 μ m; 22 striae in 10 μ m, 12 fibulae in 10 μ m. Although this diatom resembles some modern *Fragilariopsis* species (See Harwood et al., 1989a, for discussion), SEM examination of this taxon from Ross Ice Shelf Project sample 45-CC (Scherer, unpublished data) reveals simple striae, as opposed to the doubled (dicussate) areolae pattern characteristic of most modern *Fragilariopsis* species. This occurrence may represent the oldest record of this important genus. (Pl. 1, Figs. 28-31)

Genus et sp. uncertain A of Harwood et al., 1998.

Comments: This morphotype occurs as fragments between 111.05 to 80.65 mbsf.

***Goniothecium* spp.** Comments: Most of the specimens of *Goniothecium* identified in this study were of *G. odontella* (Pl. 3, Fig. 14), with rare occurrence of *G.*

decoratum.

***Grammatophora* spp.** (Pl. 2, Fig. 20)

Hemiaulus dissimilis Grove & Sturt. (Pl. 3, Figs. 12-13)

Hemiaulus polycystinorum Ehrenberg. Comments: This diatom occurs sporadically between 158 and 483.92 mbsf. (Pl. 3, Fig. 17)

***Hemiaulus* sp. A** of Harwood, 1986, p. 86, pl. 3, figs. 12 and 19. Description: Valve oval, lightly silicified; long axis 19 – 25 μ m long; areolae variable in size, 7 in 10 μ m; elevations narrow, 25 μ m long, mostly hyaline, with vertical lines of pores; small connecting spine on the external side of each elevation; margin is rarely preserved. (Pl. 3, Fig. 15)

***Hemiaulus* sp. B.** Comments: This diatom was noted in a sample at 474.90 mbsf. (Pl. 3, Fig. 16)

***Hemiaulus* sp. C; *Hemiaulus polycystinorum* sensu Harwood, 1989 (in part), pl. 4, fig. 13; Barron & Mahood, 1993 (in part), pl. 4, fig. 8. (Pl. 3, Figs. 10)**

***Hyalodiscus* spp.** Comments: This grouping includes *Hyalodiscus radiatus* var. *maximus*, among other taxa.

***Ikebea* sp. A.** Comments: This form is small and lightly-silicified; striae and marginal spines were not visible in LM observations. (Pl. 1, Fig. 25)

***Ikebea* sp. B.** Comments: This form is larger than *Ikebea* sp. A; striae and marginal spines were not visible in LM observations. (Pl. 1, Figs. 22-23)

***Ikebea* sp. C.** Comments: This form is more heavily-silicified than *Ikebea* sp. A and *Ikebea* sp. B and possesses prominent marginal spines. Striae were not visible in LM observations. (Pl. 1, Fig. 24)

***Isthmia* spp.** Comments: Fragments of *Isthmia* spp. occur throughout the cored interval.

Kannoia hastata Komura; *Ikebea tenuis* (Brun) Akiba of Harwood, 1989. (Pl. 1, Figs. 26-27)

Genus *Kisseleviella* Sheshukova-Poretskaya. Comments:

In the present study, several diatom taxa are assigned to the genus *Kisseleviella*, yet none conform with existing *Kisseleviella* taxa: *Kisseleviella carina* Sheshukova-Poretskaya (1962), *K. ezoensis* Akiba (1986), *K. magnaareolata* Akiba & Yanagisawa (1986), and *K. cuspidata* Gleser et al. (1986). Taxa previously reported as *Kisseleviella carina* from Antarctica and the Southern Ocean likely represent new species, based on differences in valve shape, position and structure of linking structures, and stratigraphical range. *Kisseleviella carina* sensu stricto, however, is linear-lanceolate and relatively broad in transapical width, with rounded, rostrate apices. It was originally described from Miocene strata on the Schmidt Peninsula of Sakhalin Island, Russia, by Sheshukova-Poretskaya (1962). It is also known from lower to middle Miocene strata of DSDP sites 192, 438, 439, and 584 in the North Pacific (Akiba, 1986; Akiba & Yanagisawa, 1986) and from upper Oligocene to middle Miocene strata of eastern Hokkaido Island, Japan (Morita et al., 1996). Specimens referred to as *Kisseleviella carina* from Eocene-Oligocene sediments in the southern high latitudes, however, have an elongate, inflated-lanceolate shape with apiculated, sub-capitate ends (see Hajós, 1976, pl. 25, figs. 5-9, & 14; Harwood, 1989, pl. 4, fig. 36; Barron & Mahood, 1993, pl. 5, fig.

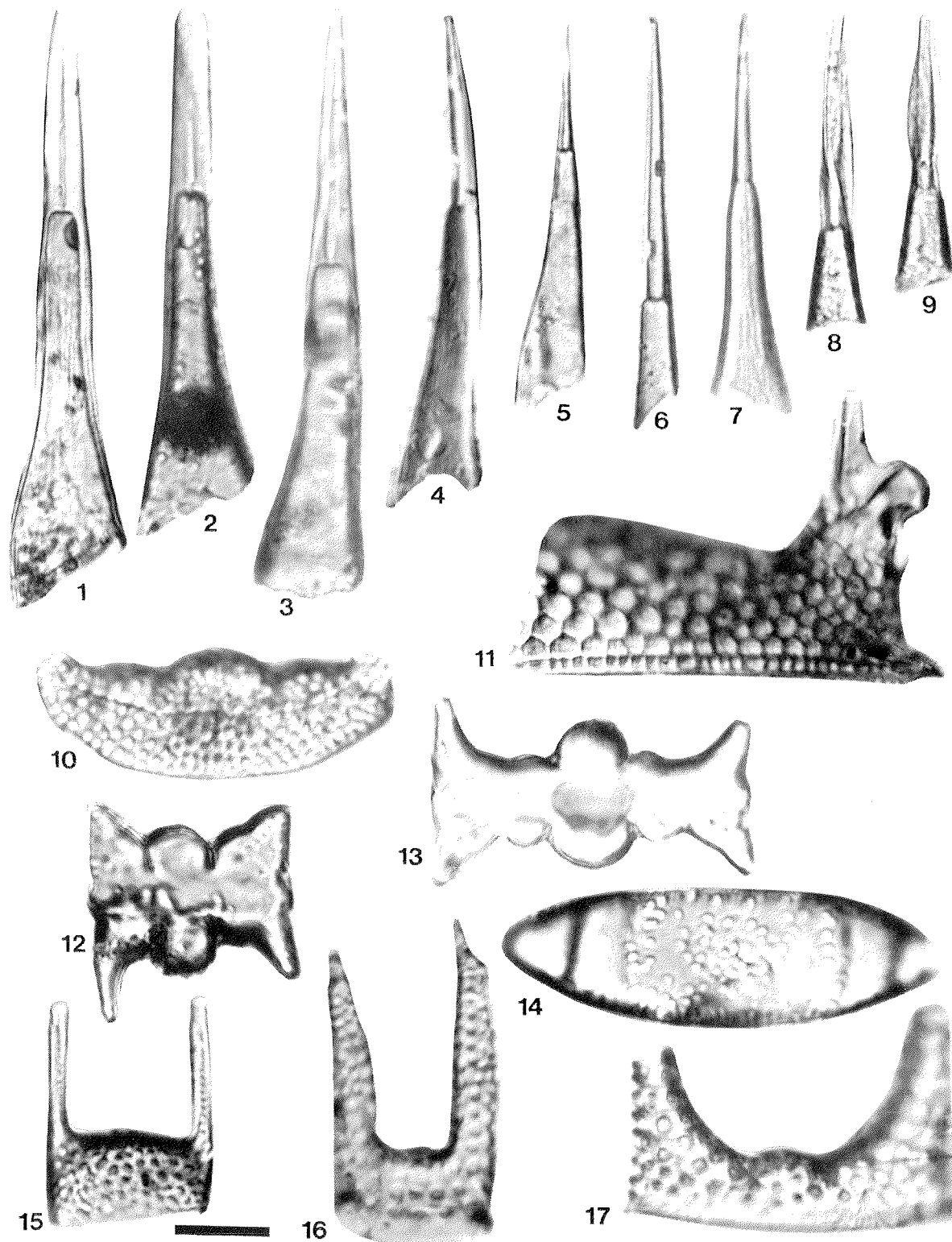


Plate 3 - Scale bar equals 10 μ m; all are valve views unless indicated otherwise.

Figures 1-2. *Rhizosolenia antarctica* Fenner; (1) CRP-2/2A-483.92-.93 m; (2) CRP-2/2A-464.98-.00 m.

Figures 3-4. *Rhizosolenia oligocaenica* Schrader; (3) CRP-2/2A-464.98-.00 m; (4) CRP-2/2A-474.90-.91 m.

Figure 5. *Rhizosolenia* sp. A; CRP-2/2A-75.52-.56 m.

Figures 6-7. *Rhizosolenia hebetata* group; (6) CRP-2/2A-75.52-.56 m; (7) CRP-2/2A-75.52-.56 m.

Figures 8-9. *Rhizosolenia* sp. B; (8) CRP-2/2A-75.52-.56 m; (9) CRP-2/2A-75.52-.56 m.

Figure 10. *Hemiaulodus* sp. C; oblique view of valve, CRP-2/2A-483.92-.93 m.

Figure 11. *Triceratium pulvinar?* Greville; Fragment, CRP-2/2A-474.90-.91 m.

Figures 12-13. *Hemiaulodus dissimilis* Grove & Sturt; (12) CRP-2/2A-564.63-.66 m; (13) CRP-2/2A-464.98-.00 m.

Figure 14. *Goniothecium odontella* Ehrenberg; Valve view, CRP-2/2A-564.63-.66 m.

Figure 15. *Hemiaulodus* sp. A of Harwood (1986); CRP-2/2A-271.02-.04 m.

Figure 16. *Hemiaulodus* sp. B; CRP-2/2A-474.90-.91 m.

Figure 17. *Hemiaulodus polycystinorum* Ehrenberg, (17) CRP-2/2A-158.50-.51 m.

11). Several distinctive taxa identified in CRP-2/2A material are presented below.

Kisseleviella sp. A; *Kisseleviella carina* Sheshukova-Poretskaya of Harwood, 1986, p. 86, pl. 6, figs. 12-15; cf. *Kisseleviella* sp. A of Akiba in Morita et al., 1996, p. 117, pl. 4, figs. 9-10. Description: Valve 15 to 40 mm in length with a maximum width of ~8 µm, faint areolae are visible on some specimens in LM; valve is rhombic-lanceolate in shape and possesses three “rings” of linking spines - one large, central (or primary) set and two smaller, lateral (or secondary) sets; each ring is centered transapically. The chief structural difference between this morphology and *Kisseleviella carina* s.s. is the presence of multi-element rings comprising the lateral sets of linking structures. *Kisseleviella* sp. A also significantly differs from *Kisseleviella carina* s.s. in valve shape (see notes above). (Pl. 1, Figs. 1-5)

Kisseleviella sp. B. Description: Valve 30 to 45 µm in length with a maximum width of ~7 µm, covered by faint pores; valve elongate with an inflated-lanceolate shape and protracted, rounded apices. Similar to *Kisseleviella* sp. A, three “rings” of linking spines are present - one large, central (or primary) set and two smaller, lateral (or secondary) sets, comprised of multiple-elements. (Pl. 1, Figs. 6-7)

Kisseleviella sp. C. Description: Valve 20 to 40 µm in length with maximum width of ~6 µm, covered by faint pores; valve is inflated-lanceolate in shape with protracted, rounded apices. The central array of linking spines is arranged in a disorganized fashion. Location of secondary or lateral linking structures is not obvious and when present represented by single elements. (Pl. 1, Figs. 8-13)

Kisseleviella sp. D. Description: Valve 10 to 15 µm in length with maximum width of ~6 µm; valve is lanceolate in shape with very slightly protracted apices. Many specimens also show a slight bilateral asymmetry with “rotated” apices. 3 to 10 linking spines arranged in a single, central ring or disorganized fashion. Location of secondary or lateral linking structures is not obvious and when present represented by single elements. *Kisseleviella* sp. C and *Kisseleviella* sp. D may represent different size cells of the same taxon. (Pl. 1, Figs. 14-17)

Kisseleviella sp. E. Description: Valve is a squat, rhombic-lanceolate shape, 10 to 15 µm in length with a maximum width of ~7 µm, covered by faint pores; 5 to 10 linking spines arranged in a single, central ring, or, on some specimens, with a disorganized, random distribution. (Pl. 1, Fig. 18)

Kisseleviella sp. F; Resting spore B of Barron & Mahood, 1993, pl. 5, figs. 17 and 19. Description: Valve is linear-lanceolate and bilaterally assymetrical in shape with sharply tapered (or apiculated) apices, ~25 µm in length with a maximum width of ~8 µm. (Pl. 1, Fig. 19)

Kisseleviella sp. G; *Kisseleviella carina* sensu Harwood, 1989 (in part), p. 79, pl. 4, fig. 37, not figs. 35, 36. Description: Valve shape is inflated-lanceolate with apiculated, sub-capitate apices, 20 to 30 µm in length with a maximum width of ~12 µm; 5 to 10 central linking spines are arranged in a single, offset ring, or

in a random distribution. Secondary or lateral linking spines consist of a single “post-and-crown” (or spiny and annular tubercle) structure, and are bilaterally offset. (Pl. 1, Figs. 20-21)

Lisitzinia ornata Jousé; Harwood, 1989, p 79, pl. 5, fig. 6. (Pl. 2, Fig. 2)

Lisitzinia ornata f. pentagona Harwood. (Pl. 2, Fig. 1)

Navicula? spp.

Navicula sp. cf *N. udentsevii* Schrader & Fenner. (Pl. 5, Fig. 6)

Odontella spp.

Paralia sulcata (Ehrenberg) Cleve.

Pinnularia spp. Comments: Specimens of an unknown *Pinnularia* spp. occur in two samples at 80.65 and 264.38 mbsf.

Proboscia aff. *praebarboi* (Schrader) Jordan & Priddle.

Proboscia spp.

Pseudopyxilla americana (Ehrenberg) Forti.

Pseudopyxilla sp. A of Harwood, 1989, pl. 3, fig. 17. Comments: This morphology occurs in one sample at 483.92 mbsf.

Pseudotriceratum radiosoreticulatum Grunow in Van Heurck. (Pl. 4, Fig. 3)

Pterotheca reticulata Sheshukova-Poretskaya; Harwood, 1986, p. 86, pl. 6, fig. 20-23. (Pl. 5, Figs. 4, 13)

Pterotheca? sp. A; Schrader & Fenner, 1976, pl. 43, fig. 14. (Pl. 6, Fig. 6)

Pyrgopyxis eocena Hendy. (Pl. 5, Fig. 9)

Pyxilla reticulata Grove & Sturt.

Radialiplicata clavigera (Grunow in Van Heurck) Gleser. (Pl. 6, Fig. 7)

Rhabdonema japonicum Tempère & Brun (Pl. 5, Fig. 10).

Rhabdonema sp. cf *R. elegans* Tempère & Brun. Harwood, 1989, p. 80. Comments: Occurrence was noted in one sample at 111.05 mbsf. (Pl. 5, Fig. 12)

Rhabdonema sp. A of Harwood, 1989, pl. 6, figs. 7-8.

Rhabdonema spp. / *Grammatophora* spp. (Pl. 2, Fig. 17)

Raphoneis amphiceros (Ehrenberg) Ehrenberg (Pl. 2, Fig. 13)

Rhizosolenia antarctica Fenner, 1984, p. 333, pl. 2, fig. 5. (Pl. 3, Figs. 1-2)

Rhizosolenia hebetata Bailey group. (Pl. 3, Figs. 6-7)

Rhizosolenia oligocaenica Schrader. (Pl. 3, Figs. 3-4)

Rhizosolenia sp. A. Comments: The valve shape of *Rhizosolenia* sp. A resembles a small, lightly-silicified *R. oligocaenica*. (Pl. 3, Fig. 5)

Rhizosolenia sp. B. Comments: Specimens of *Rhizosolenia* sp. B possess a distinctive twist on the spine. (Pl. 3, Figs. 8-9)

Rhizosolenia sp. C of Harwood, 1989, pl. 3, fig. 25. Comments: This form was noted in one sample at 483.92 mbsf.

Rocella praenitida (Fenner) Fenner. (Pl. 5, Fig. 2)

Rouxia granda Schrader in Schrader & Fenner. Comments: Rare specimens of this taxon was noted in samples between 564.63 and 542.04 mbsf.

Rouxia obesa Schrader.

Rouxia sp. A Description: A long and slender *Rouxia* morphology was observed as fragments at 271.02 and 292.08 mbsf.

Sceptroneis spp. Comments: Several specimens of

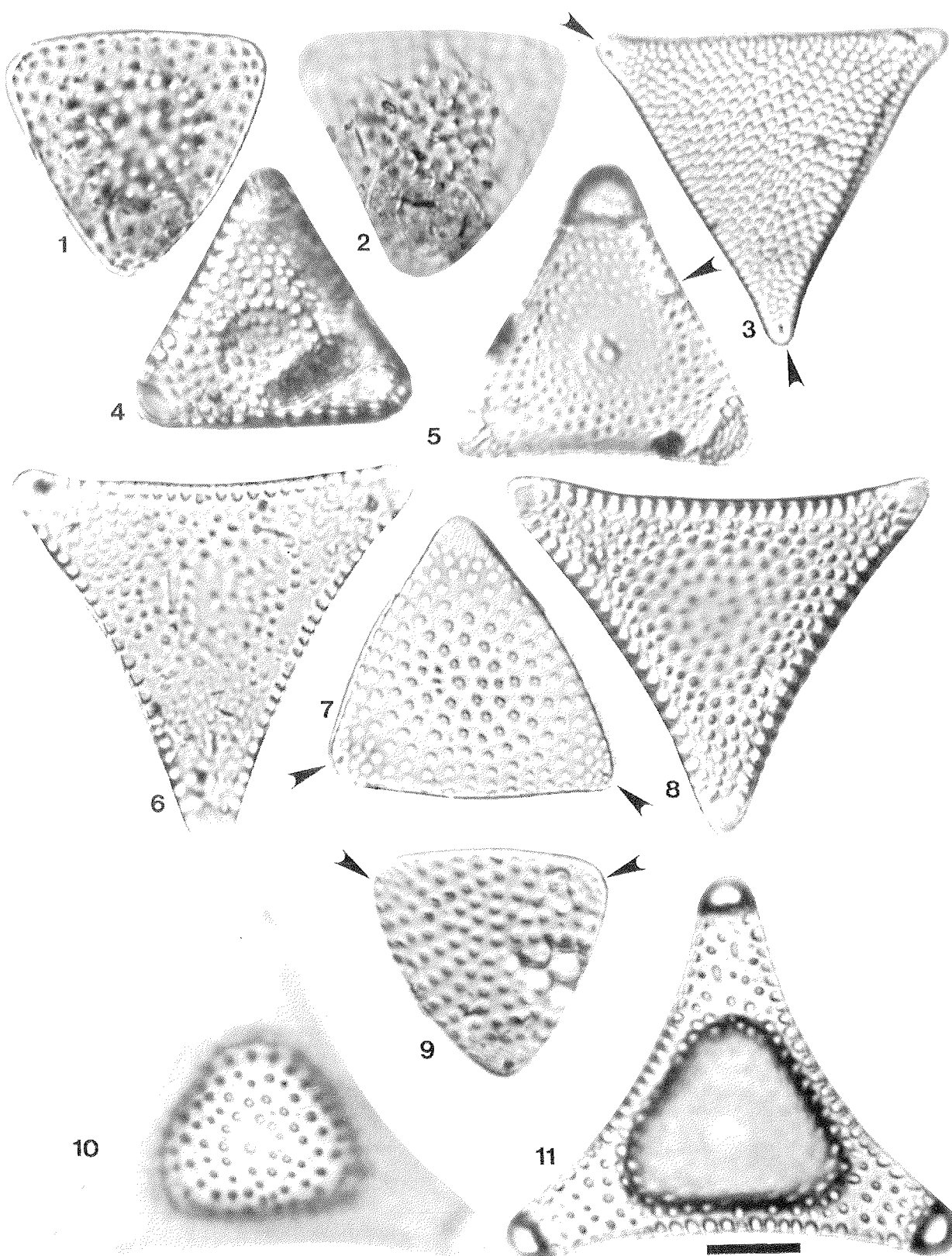


Plate 4 - Scale bar equals 10 μm ; all are valve views unless indicated otherwise.

Figures 1-2. *Eurossia irregularis* var. *irregularis* centrally swollen hypovalve (1-2) Low/ high focus, CRP-2/2A-474.90-.91 m.

Figure 3. *Pseudotriceratum radiosoreticulatum* (Grunow in Van Heurck) Fenner; CRP-2/2A-483.92-.93 m (arrows denote positions of labiate processes; labiate process on third arm is present but not visible in photograph).

Figure 4. *Trinacria* sp. A; CRP-2/2A-292.08-.10 m.

Figure 5. *Trinacria* sp. B; CRP-2/2A-264.38-.39 m (arrow denotes position of labiate process).

Figures 6?, 10, 11. *Trinacria racovitzae* Van Heurck; (6) CRP-2/2A-271.02-.04 m; (10, 11) high/ low focus, CRP-2/2A-292.08-.10 m.

Figures 7, 9. *Eurossia irregularis* var. *irregularis* (Greville) Sims; (7) CRP-2/2A-464.98-00 m; (9) CRP-2/2A-474.90-.91 m (arrows denote positions of labiate processes).

Figure 8. *Trinacria excavata* Heiberg; 57.32-42 m.

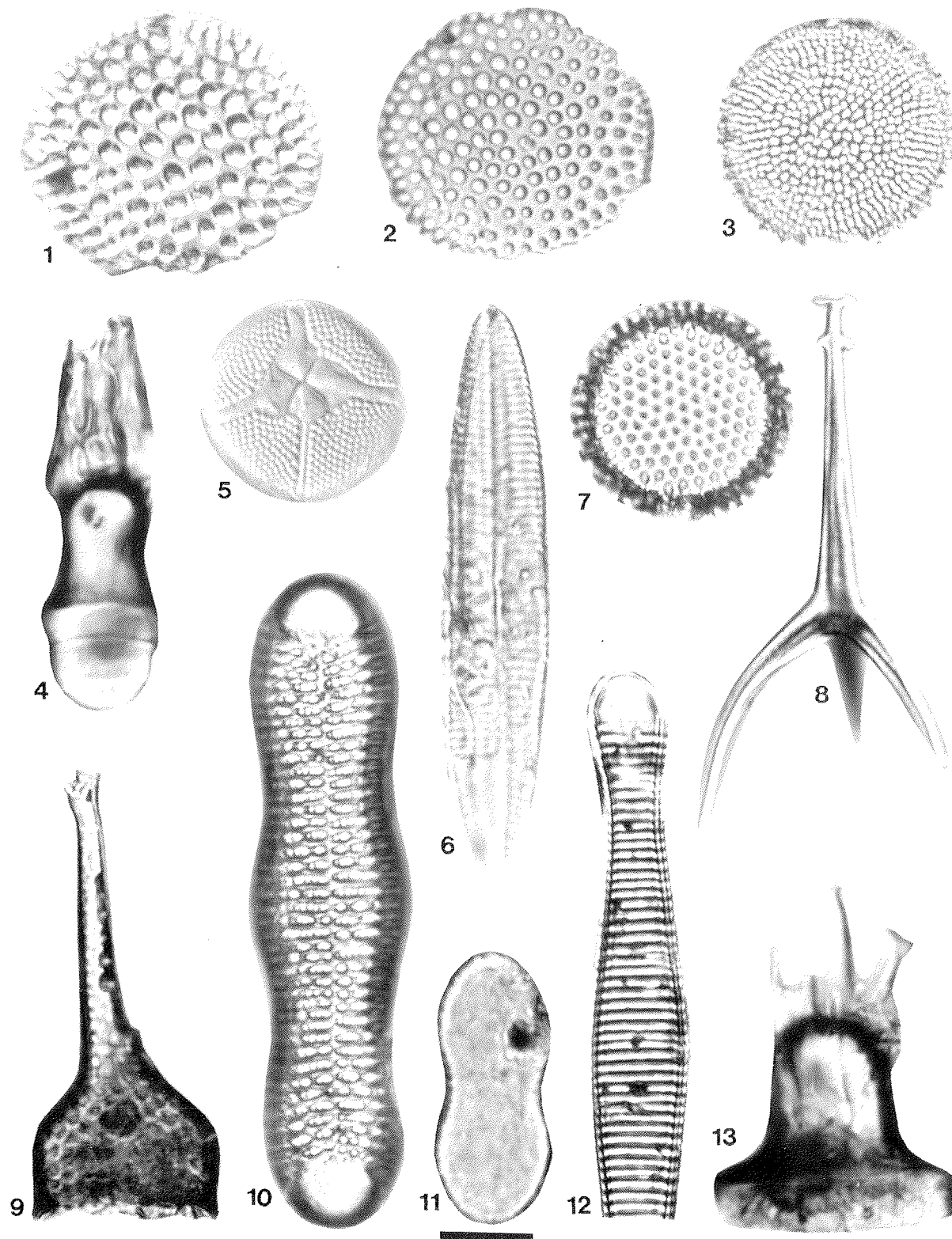


Plate 5 - Scale bar equals 10 μm ; all are valve views unless indicated otherwise.

- Figure 1. *Coscinodiscus* sp. cf. *C. marginatus* Ehrenberg; CRP-2/2A-122.56-.57 m.
- Figure 2. *Rocella praenitida* (Fenner) Fenner; CRP-2/2A-130.90-.92 m.
- Figure 3. *Thalassiosira nansenii* Scherer in Scherer & Koç; (3) CRP-2/2A-71.13-.14 m.
- Figures 4, 13. *Pterotheca reticulata* Sheshukova-Poretzkaya; (4) CRP-2/2A-464.98-00 m; (13) CRP-2/2A-271.02-.04 m.
- Figure 5. *Asteromphalus* sp. A; CRP-2/2A-71.13 m.
- Figure 6. *Navicula* cf. *undintsevii* Schrader & Fenner; CRP-2/2A-236.25-.26 m.
- Figure 7. *Stephanopyxis oamaruensis* Hajós; CRP-2/2A-483.92-.93 m.
- Figure 8. *Calicipediniun* sp. A (endoskeletal dinoflagellate); CRP-2/2A-271.02-.04 m.
- Figure 9. *Pyrgopyxix eocena* Hendey; CRP-2/2A-474.90-.91 m.
- Figure 10. *Rhabdonema japonicum* group Tempère & Brun; CRP-2/2A-57.32-.42 m.
- Figure 11. *Chaetoceros panduriformis* (Pantocsek) Gombos; CRP-2/2A-292.08-.10 m.
- Figure 12. *Rhabdonema* sp. cf. *R. elegans* Tempère & Brun; CRP-2/2A-474.90-.91 m.

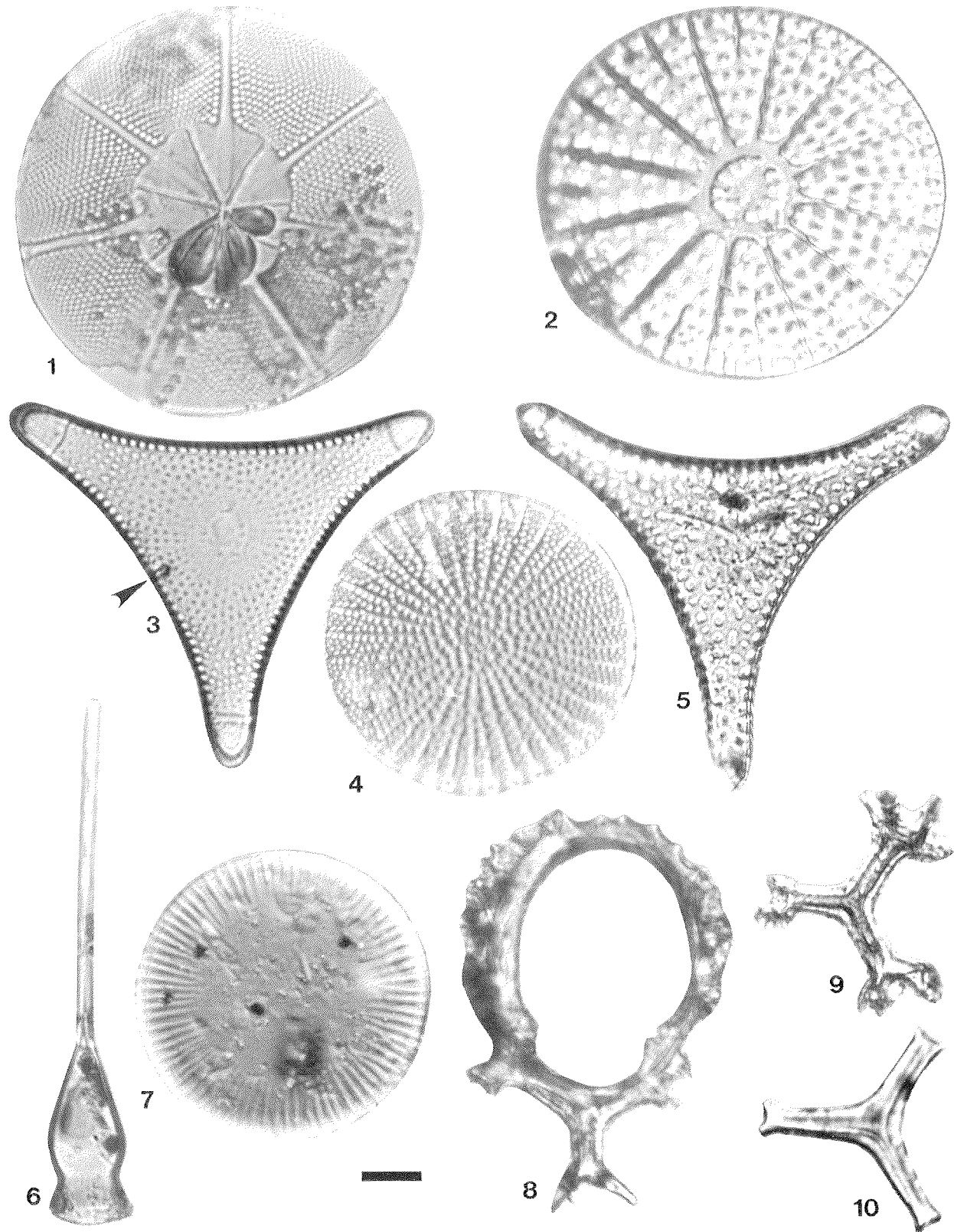


Plate 6 - Scale bar equals 10 μm ; all are valve views unless indicated otherwise.

Figure 1. *Asterolampra punctifera* (Grove) Hanna; CRP-2/2A-464.98-00 m.

Figure 2. *Arachnoidiscus cf. sendaicus* Brown; CRP-2/2A-215.72-.74 m.

Figure 3. *Trinacria* sp.; CRP-2/2A-264.38-.39 m (arrow denotes position of prominent labiate process).

Figure 4. *Stictodiscus hardmanianus* Greville; CRP-2/2A-111.05-.06 m.

Figure 5. *Trinacria excavata* Heiberg; CRP-2/2A-271.02-.04 m.

Figure 6. *Pterotheca?* sp. A; CRP-2/2A-474.90-.91 m.

Figure 7. *Radialiplicata clavigera* (Grunow) in Van Heurck Gleser; CRP-2/2A-474.90-.91 m.

Figures 8-10. *Falsebria ambigua* Deflandre / *Hovasebria brevispinosa* (Hovasse) Deflandre group (ebridians); (8) CRP-2/2A-271.02-.04 m; (9) CRP-2/2A-271.02-.04 m; (10) CRP-2/2A-413.05-.06 m.

Sceptroneis spp. were noted at 271.02 and 264.38 mbsf. *Skeletonemopsis mahoodii* Sims; *Skeletonemopsis barbadensis* sensu Barron & Mahood, 1993; sensu Cape Roberts Science Team, 1999. (Pl. 2, Figs. 8-12) *Stellarima microtrias* Hasle & Sims.

Stephanopyxis eocaenica Hajós.

Stephanopyxis hyalomarginata Hajós.

Stephanopyxis oamaruensis Hajós. (Pl. 5, Fig. 7)

Stephanopyxis spinossissima Grunow.

***Stephanopyxis* spp.** Comments: This group includes many distinct, mostly long-ranging forms, including *S. turris* (Greville & Arnott) Ralfs in Prichard, *S. grunowii* Grove & Sturt, among others.

Stictodiscus hardmanianus Greville. Comments: Specimens of this taxon were noted at 111.05 and 483.92 mbsf. (Pl. 6, Fig. 4)

Thalassiosira nansenii Scherer in Scherer & Koç. (Pl. 5, Fig. 3)

Thalassiosira praefraga Gladkov & Barron; *Thalassiosira fraga* Schrader, in Harwood et al., 1989a, pl. 2, fig. 3; *Coscinodiscus* sp. 1 of McCollum, 1975, p. 526, pl. 8, fig. 3. (Pl. 2, Figs. 3, 7)

Thalassiosira mediaconvexa Schrader & Fenner.

Genus "Tigeria" Comments: "Tigeria" is an informal working genus name for a group of diatoms pending formal designation, following study of morphological characters in the SEM.

"Tigeria" sp. A. Comments: This taxon was previously reported as *Synedra?* sp. 1 Brady, 1980; Harwood et al., 1989a; *Tetracyclus* sp. of Harwood, 1986, pl. 7, figs. 34, 37, 38, not figs 40, 41; *Synedra/Fragilaria* sp. A. of Harwood, 1989, p. 81. Description: Valve lanceolate-capitate, 20 - 24 μ m long, with 8 – 9 striae in 10 μ m; striae comprised of simple pores in short, discontinuous lines. No processes were observed in the light microscope. (Pl. 2, Fig. 14)

"Tigeria" sp. B. Comments: This taxon was previously reported as *Synedra?* sp. 2 of Brady, 1980; Harwood et al., 1989a. Description: Valve lanceolate to narrow-elliptical, 23 - 30 μ m in length, 4 - 7 μ m wide; striae as in "Tigeria" sp. A. No processes were observed in the light microscope. (Pl. 2, Fig. 15)

"Tigeria" sp. C. Comments: This taxon has not been previously reported, but is known to occur commonly in materials recovered from beneath the Ross Ice Shelf (RISP) (Harwood et al., 1989a; Scherer, 1992; Scherer, unpublished data). Description: Valve, oval, 9 - 14 μ m in length, nearly all hyaline, with a single line of marginal pores, instead of striae. No labiate processes were observed in SEM evaluation of this taxon in RISP material, though each apex possesses one or two pores. Due to the small size and indistinct structure, this diatom is easily overlooked. (Pl. 2, Fig. 16)

Triceratium pulvinar? Schmidt. (Pl. 3, Fig. 11)

Trigonium arcticum (Brightwell) Cleve. Comments: Fragments of this taxon were noted throughout the recovered section in CRP-2/2A.

Trinacria excavata Heiberg. (Pl. 4, Fig. 8; Pl. 6, Fig. 5)

Trinacria* sp. cf. *T. pileolus (Ehrenberg) Grunow.

Trinacria racovitzae Van Heurck. (Pl. 4, Figs. 6, 10, 11)

***Trinacria* sp. A.** Comments: This morphotype may

belong to genus *Sheshukovia* Gleser. (Pl. 4, Fig. 4)

***Trinacria* sp. B.** Comments: This morphotype possesses a prominent labiate process on the margin, and may belong to the genus *Sheshukovia* Gleser. It was noted at 264.38 mbsf in CRP-2/2A. (Pl. 4, Figs. 5)

***Trinacria* sp.** (Pl. 6, Fig. 3)

Trochosira coronata Schrader & Fenner.

Trochosira spinosus Kitton. (Pl. 2, Figs. 4-6)

Vulcanella hanuiae Sims & Mahood, 1998, p. 115, figs. 1-12, 44-48; *Cotyledon fogedi* (Hendey) Harwood, 1989; *Tumulopsis fogedi* Hendey sensu Barron & Mahood, 1993 p. 44, pl. 2, figs. 7, 9, 10.

SILICOFLAGELLATES

Corbisema apiculata (Lemmermann) Hanna.

Corbisema triacantha (Ehrenberg) Hanna.

Dictyocha deflandrei Frenguelli ex Glezer.

Dictyocha frenguelli Deflandre.

Dictyocha pentagona (Schulz) Bukry & Foster.

Distephanus quinquangellus Bukry & Foster.

Distephanus speculum (Ehrenberg) Haeckel.

Septamesocena apiculata apiculata (Schulz) Bachmann.

Septamesocena pappii (Bachmann) Desikachary & Prema.

Comments: *Septamesocena pappii* is identified by the presence of two radial spines, oriented at ~90° relative to one another, that emanate from each corner of the basal ring. A variety of *Septamesocena pappii* with one reduced radial spine (in length) on each basal-ring corner is noted in the lowermost Miocene of the CRP-2/2A drillcore.

EBRIDIANS

Ammodochium rectangulare (Schulz) Deflandre.

Comments: In addition to single-skeleton morphologies, a double skeleton morphology of *Ammodochium rectangulare* with medial silicification is also noted in the CRP-2/2A drillcore. See Bohaty & Harwood (2000) for illustrations of several varietal forms of *Ammodochium rectangulare*.

Falsebria ambigua Deflandre. Comments: *Falsebria ambigua* is a rudimentary ebridian morphology with three radiating elements, in the same plane, joined at 120°. Some overlap exists in the taxonomic definition of *Falsebria ambigua* and *Hovassebria brevispinosa*. Two of the elements in *Hovassebria brevispinosa* are commonly closed by a loop, and the loop is absent in *Falsebria ambigua*. See Bohaty & Harwood (2000) for additional discussion. (Pl. 6, Figs. 8-10)

Pseudammodochium lingii Bohaty & Harwood, 2000.

Pseudammodochium sphericum Hovasse. Comments: Both single and double-skeleton morphologies of *Pseudammodochium sphericum* are noted in the CRP-2/2A drillcore.

ENDOSKELETAL DINOFLAGELLATES

Carduifolia gracilis Hovasse.

***Calicipedinium* sp. A.** Comments: A small, Y-shaped endoskeletal dinoflagellate is noted in upper Oligocene

to lower Miocene sections of the CRP-2/2A drillcore. This morphology possesses three radial elements which each terminate with a sharp point. (Pl. 5, Fig. 8). Dumitrica (1973) describes two taxa in the genus *Calicipedinium* as endoskeletal dinoflagellates, but morphologies placed in this genus may also be sponge spicules or have another unknown affinity. Similar morphologies to those described by Dumitrica (1973) are noted in the upper Oligocene to lower Miocene section of the CRP-2/2A drillcore and are designated as *Calicipedinium* sp. A. Complete specimens consist of an axial element (or rod) with a small apical cup or disc. Three downward-pointing elements radiate from the base of the axial rod and each possess a median crest and terminate with a sharp point. Broken specimens of this morphology are commonly Y-shaped.

CHRYSOPHYTE CYST

Archaeosphaeridium tasmaniae Perch-Nielsen.

OTHER SILICEOUS FLAGELLATE

Macrora barbadensis (Deflandre) Bukry.

ACKNOWLEDGEMENTS

Support for the Cape Roberts Project comes from the international consortium consisting of the national research programs of US, New Zealand, Italy, Germany, UK and Australia. Support for this research came from NSF grant OPP-9420062 to DMH and RPS. RPS received additional support from the Swedish Natural Sciences Research Council (NFR). John Barron and Andrew McMinn reviewed the manuscript and provided many useful comments. We offer our special thanks to Rusty Divine for his tremendous assistance in sample preparation on the ice, and for his unbounded good cheer.

REFERENCES

- Akiba F., 1986. Middle Miocene to Quaternary diatom biostratigraphy in the Nakai trough and Japan trench, and modified lower Miocene to Quaternary diatom zones for middle-to-high latitudes of the North Pacific. In: Kagami H., Karig D.E., Caulbourn W.T. et al. (eds.), *Initial Reports of the Deep Sea Drilling Project*, Washington, U.S. Government Printing Office, **87**, 393-481.
- Akiba F. & Yanagisawa Y., 1986. Taxonomy, morphology and phylogeny of the Neogene diatom zonal marker species in the middle-to-high latitudes of the North Pacific. In: Kagami H., Karig D.E., Caulbourn W.T. et al. (eds.), *Initial Reports of the Deep Sea Drilling Project*, Washington, U.S. Government Printing Office, **87**, 483-544.
- Akiba F., Hiramatsu C. & Yanagisawa Y., 1993. A Cenozoic diatom genus *Cavittatus* Williams; an emended description and two new biostratigraphically useful species, *C. lanceolatus* and *C. rectus* from Japan. *Bull. Natn. Sci. Mus., Tokyo*, Ser. C, **19**(1), 11-39.
- Baldauf J.G. & Barron J.A., 1991. Diatom biostratigraphy: Kerguelan Plateau and Prydz Bay regions of the Southern Ocean. In: Barron J.A., Larsen B. et al. (eds.), *Proceedings of the Ocean Drilling Program, Scientific Results*, College Station, TX (Ocean Drilling Program), **119**, 547-598.
- Barron J.A. & Mahood A.D., 1993. Exceptionally well-preserved early Oligocene diatoms from glacial sediments of Prydz Bay, East Antarctica. *Micropaleontology*, **39**(1), 29-45.
- Berggren W.A., Kent D.V., Swisher C.C. III & Aubrey M.-P., 1995. A revised Cenozoic geochronology and chronostratigraphy. In: Berggren W.A., Kent D.V., Aubrey M.-P. & Hardenbol J.A. (eds.), *Geochronology, Time Scales, and Global Stratigraphic Correlation*, SEPM Special Publication, **54**, 129-212.
- Bohaty S.M. & Harwood D.M., 2000. Ebridian and silicoflagellate biostratigraphy from Eocene McMurdo erratics and the Southern Ocean. In: Stilwell J.D. & Feldmann R.M. (eds.), *Paleobiology and Paleoenvironments of Eocene Fossiliferous Erratics, McMurdo Sound, Antarctica*, Antarctic Research Series, American Geophysical Union, v. **76**, 99-159.
- Brady H., 1980. Palaeoenvironmental and biostratigraphic studies in the McMurdo and Ross Sea regions, Antarctica. Thesis. Macquarie University, Sydney. 235 pp.
- Brown N.E., 1933. *Arachnoidiscus*. London, W. Watson & Sons, 103 pp.
- Cape Roberts Science Team, 1999. Studies from the Cape Roberts Project, Ross Sea, Antarctica: Initial Report on CRP-2/2A. *Terra Antarctica*, **6**(1/2), 1-173.
- Cape Roberts Science Team, 2000. Studies from the Cape Roberts Project, Ross Sea, Antarctica: Initial Report on CRP-2/2A. *Terra Antarctica*, **7**(1/2), 1-209.
- Dumitrica P., 1973. Cenozoic endoskeletal dinoflagellates in southwestern Pacific sediments cored during Leg 21 of the DSDP. In: Burns R.E., Andrews J.E. et al., *Initial Reports of the Deep Sea Drilling Project*, U.S. Government Printing Office, Washington, D.C., **21**, 819-835.
- Fenner, J., 1984. Eocene-Oligocene planktic diatom stratigraphy in the low latitudes and the high southern latitudes. *Micropaleontology*, **30**, 319-342.
- Fenner J., 1985. Late Cretaceous to Oligocene planktic diatoms. In: Bolli H.M., Saunders J.B. & Perch-Nielsen K. (eds.), *Plankton Stratigraphy*, Cambridge University Press, pp. 713-762.
- Gladenkov A.Y. & Barron J.A., 1995. Oligocene and early middle Miocene diatom biostratigraphy of Hole 884B. In: Rea D.K., Basov I.A., Scholl D.W. & Allan J.F. (eds.), *Proceedings of the Ocean Drilling Program, Scientific Results*, College Station, TX (Ocean Drilling Program), **145**, 21-41.
- Gleser S.I., Dolmatova L.M. & Lupikina E.G., 1986. Marine Paleogene diatom algae from eastern Kamchatka. *Bot. Jour.*, **71**(7), 851-859.
- Gombos A.M., 1977. Paleogene and Neogene diatoms from the Falkland Plateau and Malvinas Outer Basin. In: Barker P.F., Dalziel I.W.D. et al. (eds.), *Initial Reports of the Deep Sea Drilling Project*, Washington, U.S. Government Printing Office, **36**, 575-687.
- Gombos A.M. & Ciesielski P.F., 1983. Late Eocene to early Miocene diatoms from the southwest Atlantic. In: Ludwig W.J., Krasheninikov V.A. et al. (eds.), *Initial Reports of the Deep Sea Drilling Project*, Washington (U.S. Government Printing Office), **71**, 583-634.
- Hajós M., 1976. Upper Eocene and lower Oligocene diatomaceae, archaeomonadaceae, and silicoflagellatae in southwestern Pacific sediments, DSDP Leg 29. In: Hollister C.D., Craddock C. et al. (eds.), *Initial Reports of the Deep Sea Drilling Project*, Washington, U.S. Government Printing Office, **35**, 817-884.
- Hanna G.D., Hendy N.I., & Brigger A.L., 1976. Some Eocene diatoms from South Atlantic cores, Part 1: New and rare species of *Arachnoidiscus*. *Occasional Papers of the California Academy of Sciences*, **123**, 1-20.
- Harwood D.M., 1986. Diatoms. In: Barrett P.J. (ed.), *Antarctic Cenozoic History from the MSSTS-1 Drillhole, McMurdo Sound, DSIR Bulletin*, **237**, 69-107.
- Harwood D.M., 1989. Siliceous microfossils. In: Barrett P.J. (ed.) *Antarctic Cenozoic History from the CIROS-1 Drillhole, McMurdo Sound, DSIR Bulletin*, **245**, 67-97.
- Harwood D.M. & Maruyama T., 1992. Middle Eocene to Pleistocene diatom biostratigraphy of Southern Ocean sediments from the Kerguelan Plateau, Leg 120. In: Wise S.W. Jr., Schlüch R. et al. (eds.), *Proceedings of the Ocean Drilling Program, Scientific Results*, College Station, TX, Ocean Drilling Program, **120** (2), 683-733.
- Harwood D.M. & Bohaty S.M., 2000. Marine diatom assemblages from Eocene and younger erratics, McMurdo Sound, Antarctica. In: Stilwell J.D. & Feldmann R.M. (eds.), *Paleobiology and Paleoenvironments of Eocene Fossiliferous Erratics, McMurdo Sound, Antarctica*, Antarctic Research Series, American Geophysical Union, v. **76**, 73-98.
- Harwood D.M., Scherer R.P. & Webb P.-N., 1989a. Multiple Miocene productivity events in West Antarctica as recorded in upper Miocene sediments beneath the Ross Ice Shelf (Site J-9). *Marine Micropaleontology*, **15**, 91-115.
- Harwood D.M., Barrett P.J., Edwards A.R., Rieck H.J. & Webb P.-N., 1989b. Biostratigraphy and chronology. In: Barrett P.J. (ed.),

- Antarctic Cenozoic History from the CIROS-I Drillhole, McMurdo Sound, DSIR Bulletin*, **245**, 231-239.
- Harwood D.M., Bohaty S.M. & Scherer R.P., 1998. Lower Miocene diatom biostratigraphy of the CRP-I drillcore, McMurdo Sound, Antarctica. In: Hambrey M.J. & Wise S.W. (eds.), *Terra Antarctica*, **5**(3), 499-514.
- Hasle G.R., von Stosch A. & Syvertsen E., 1983. Cymatosiraceae, a new diatom family. *Bacillaria*, **6**, 9-156.
- Kellogg D.E. & Kellogg T.B., 1986. Diatom biostratigraphy of sediment cores from beneath the Ross Ice Shelf. *Micropaleontology*, **32**, 74-79.
- Mahood A.D., Barron J.A. & Sims P.A., 1993. A study of some unusual, well-preserved Oligocene diatoms from Antarctica. *Nova Hedwigia, Beiheft*, **106**, 243-267.
- McCollum D.W., 1975. Diatom stratigraphy of the Southern Ocean. In: Hayes D.E., Frakes L.A., et al. *Initial Reports of the Deep Sea Drilling Project*, Washington, U.S. Govt. Printing Office, **28**, 515-571.
- Morita R., Titova L.V. & Akiba F., 1996. Oligocene-early Miocene molluscs and diatoms from the Kitami-Tsubetsu area, eastern Hokkaido, Japan. *Science Reports of the Tohoku University, Sendai, Second Series (Geology)*, **63**(2), 53-213.
- Ramsay A.T.S. & Baldauf J.G., 1999. *A Reassessment of the Southern Ocean Biochronology*. Geological Society, London, Memoir **18**, 122 pp.
- Roberts A.P., Wilson G.S., Florindo F., Sagnotti L., Verosub K.L. & Harwood, D.M., 1998. Magnetostratigraphy of lower Miocene strata from the CRP-I core, McMurdo Sound, Ross Sea, Antarctica. *Scientific Results of the Cape Roberts Drilling Project*, **5**(3), 703-713.
- Round F.E., Crawford R.M., & Mann D. G., 1990. *The Diatoms*. Cambridge University Press, Cambridge, U.K., 774pp.
- Scherer R.P., 1992. Diatom paleoproductivity and sediment transport in West Antarctic basins and the Neogene History of the West Antarctic Ice Sheet. Ph.D. Dissertation, The Ohio State University, Columbus, 276pp.
- Scherer R.P. & Koç N., 1996. Late Paleogene diatom biostratigraphy and paleoenvironments of the northern Norwegian-Greenland Sea. In: Thiede J., Myhre A.M., Firth J.V., Johnson G.L., & Ruddiman W.F. (eds.), *Proceedings of the Ocean Drilling Program, Scientific Results*, College Station, TX, Ocean Drilling Program, **151**, 75-99.
- Schrader H.-J., 1976. Cenozoic planktonic diatom biostratigraphy of the Southern Pacific Ocean. In: Hollister C.D., Craddock C. et al. (eds.), *Initial Reports of the Deep Sea Drilling Project*, Washington, U.S. Govt. Printing Office, **35**, 605-672.
- Schrader H.-J. & Fenner J., 1976. Norwegian Sea Cenozoic diatom biostratigraphy and taxonomy. In: Talwani M., Udintsev G. et al. (eds.), *Initial Reports of the Deep Sea Drilling Project*, Washington, U.S. Government Printing Office, **38**, 921-1099.
- Sheshulova-Poretskaya V.S., 1962. New and rare Bacillariophyta from the diatom suite of north Sakhalin. *Uchenyye Zapiski, Seriya Biologicheskii Nauk*, Leningrad State University, Biological Institute, **49**(313), 203-211.
- Sims P. A. & Mahood A., 1998. *Vulcanella hannaee* Sims and Mahood, gen. et sp. nov., with a discussion of the genera *Tumulopsis* Hendy, *Acanthodiscus* Pantocsek, *Poretzkia* Jouse and *Goniothecium* Ehrenberg. *Diatom Research*, **13** (1), 113-131.
- Wilson G.S., Roberts A.P., Verosub K.L., Florindo F. & Sagnotti L., 1998. Magnetobiostratigraphic chronology of the Eocene-Oligocene transition in the CIROS-I core, Victoria Land Margin, Antarctica: Implications for Antarctic glacial history. *GSA Bulletin*, **110**, 35-47.
- Yanagisawa Y. & Akiba F., 1998. Refined Neogene diatom biostratigraphy for the northwest Pacific around Japan, with an introduction of code numbers for selected diatom biohorizons. *The Journal of the Geological Society of Japan*, **104**(6), 395-414.
- Zielinski U., 1997. Parmales (siliceous marine nanoplankton) in surface sediments of the Weddell Sea, Southern Ocean: indicators for sea ice environment? *Marine Micropaleontology*, **32**, 387-395.